



DEPARTMENT OF THE AIR FORCE  
AIR FORCE RESEARCH LABORATORY  
WRIGHT-PATTERSON AIR FORCE BASE OHIO 45433

5 June 2001

MEMORANDUM FOR US EPA  
NCEA (MD-52)  
RTP, NC 27711  
ATTN: ANNIE M. JARABEK

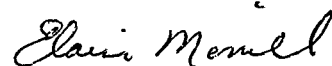
FROM: Elaine Merrill  
AFRL/HST  
Operational Toxicology Branch  
2856 G St, Bldg 79  
Wright-Patterson AFB, OH 45433-7400

SUBJECT: Consultative Letter, AFRL-HE-WP-CL-2001-0008, PBPK Model for Perchlorate-Induced Inhibition of Radioiodide Uptake in Humans.

1. This letter updates a physiologically-based pharmacokinetic (PBPK) model for predicting the inhibition of thyroid iodide uptake in humans after exposure to perchlorate ( $\text{ClO}_4^-$ ), as presented in the Consultative Letter, AFRL-HE-WP-CL-2000-0036, Human PBPK Model for Perchlorate Inhibition of Iodide Uptake in the Thyroid. The current model reflects a new model structure and incorporates unpublished data courtesy of Dr. M. Greer (Oregon Health Science University, Portland, OR), Dr. G. Goodman (Intertox, Inc., Seattle, WA), Dr. G. Brabant and Dr. H. Leitolf (Medizinische Hochschule, Hanover, Germany). Nonlinear saturable uptakes are described for the thyroid, skin and stomach compartments. The stomach and thyroid consist of three sub-compartments representing the stroma, follicle and colloid in the thyroid, or the capillary bed, stomach wall and contents in the case of the stomach. The skin contains two sub-compartments for capillaries and skin tissue. Compartments for plasma, kidney, liver, fat, richly perfused and slowly perfused tissues were described using passive diffusion. The plasma compartment for perchlorate is composed of plasma and plasma proteins to simulate binding, whereas the plasma compartment for iodide does not include binding.

2. The model adequately simulates serum concentrations and cumulative urine after drinking water exposure to perchlorate spanning four orders of magnitude (0.02 to 12.0 mg/kg-day). In addition, the model adequately simulates perchlorate-induced iodide inhibition in the thyroid from doses ranging from 0.007 to 0.5 mg/kg-day. Inhibition data from higher doses were not available.

3. For further information, please contact me by phone: (937) 255-5150 ext. 3195, fax: (937) 255-1474 or e-mail: elaine.merrill@wpafb.af.mil.



ELAINE A. MERRILL  
Operational Toxicology Branch

Attachment:

1. PBPK Model for Perchlorate-Induced Inhibition of Iodide Uptake in the Human
2. Goodyear, C.: Serum Hormones (TSH, T<sub>3</sub>, T<sub>4</sub>, fT<sub>4</sub>) Statistical Report

1<sup>st</sup> Ind, AFRL/HEST

5 June 2001

MEMORANDUM FOR US EPA

ATTN: MS. ANNIE JARABEK

This letter report has been coordinated at the branch level and is approved for release.



Richard R. Stotts, DVM, Ph.D.  
Branch Chief  
Operational Toxicology Branch  
Human Effectiveness Directorate

## **PBPK Model for Perchlorate-Induced Inhibition of Radioiodide Uptake in Humans**

Elaine A. Merrill<sup>1</sup>, Rebecca A. Clewell<sup>2</sup>, Jeffrey W. Fisher<sup>3\*</sup>, Teresa R. Sterner<sup>1</sup> and  
Jeffery M. Gearhart<sup>4</sup>

<sup>1</sup>Operational Technologies Corp.  
1370 N. Fairfield Rd., Ste. A, Dayton, OH 45432

<sup>2</sup>GEOCENTERS, Inc.  
2856 G St., Bldg 79, Wright-Patterson AFB, OH 45433

<sup>3</sup>AFRL/HEST  
2856 G St., Bldg 79, Wright-Patterson AFB, OH 45433

<sup>4</sup>ManTech Environmental Technology, Inc.  
PO Box 31009, Dayton, OH 45437-009

\*Current Address: University of Georgia  
Athens, GA, USA

5 June 2001

## INTRODUCTION

Commercially the salt, ammonium perchlorate, has been produced in the U.S. since the 1940s (Fisher *et al.*, 2000). It is used primarily for its strong oxidizing properties in explosive and pyrotechnic mixtures and as an ingredient in rocket fuel. In water, perchlorate quickly dissociates and is highly mobile and stable. As a result, perchlorate contamination has been detected in several water sources in the U.S. (Urbansky and Schock, 1999). There's concern that chronic exposure to low levels of perchlorate in drinking water could induce iodide deficiencies and subsequent thyroid disorders.

The perchlorate anion ( $\text{ClO}_4^-$ ) is very similar in ionic size, shape and charge to iodide ( $\text{I}^-$ ). These shared properties allow perchlorate to interfere with the first stage of thyroid hormone genesis by competitively inhibiting the active transfer of iodide into the thyroid by the sodium-iodide symporter (NIS). The NIS is a protein that resides in the basolateral membrane of thyroid epithelial cells (Spitzweg *et al.*, 2000). NIS simultaneously transports both  $\text{Na}^+$  and  $\text{I}^-$  ions from extracellular fluid (plasma) into the thyroid epithelial cell. This process is an example of secondary active transport. Energy is provided by the electrochemical gradient of sodium across the cell membrane; the low intracellular concentration of sodium is maintained by sodium-potassium pumps (Ajjan *et al.*, 1998).

The presence of NIS is an indicator of active uptake for iodide and likewise, perchlorate. The NIS is highly expressed in thyroid epithelial cells. Lower levels of expression have also been detected in the mammary gland, salivary gland, skin, stomach and colon. Perchlorate inhibits iodide uptake in these tissues as well. However, only the thyroid has been found to organify iodide to form thyroid hormones (Ajjan *et al.*, 1998; Spitzweg *et al.*, 1998). The perchlorate-induced decline in iodide trapping in all tissues with NIS is reversible upon elimination of perchlorate.

Thyroid hormones homeostasis occurs through a complex feedback mechanism. Thyroid-stimulating hormone (TSH) is the most important regulator of NIS gene and protein expression; up-regulation of NIS stimulates iodide transport for increased hormone production. A drop in thyroid hormones signals the pituitary to produce more TSH, which in turn stimulates NIS expression. In rats, an increase in TSH and decrease in free thyroxine ( $\text{fT}_4$ ) occurs quickly after perchlorate exposure (Wyngaarden *et al.*, 1952). In humans, however, the conservation of thyroid hormones is more efficient. Studies have shown little or no change in human TSH levels after two weeks of exposure perchlorate in drinking water (Greer *et al.*, 2000; Brabant *et al.*, 1992). Therefore, the extent of chronic low level perchlorate exposure required to cause significant hormone deficiencies is not yet known.

Adequate iodide uptake for thyroid hormone production is necessary for proper brain development during the first two years of life (Laurberg *et al.*, 2000). Iodide deficiency during the fetal and neonatal period could result in abnormal physical and mental development (Porterfield, 1994). The effects of iodide deficiencies to adult populations are less dramatic.

However, in elderly adults, especially elderly women, a high occurrence of hyperthyroidism is noted in areas of mild to moderate iodine deficiency. Hyperthyroidism is easily overlooked in the elderly and, if left untreated, may lead to cardiac arrhythmias, impaired cardiovascular reserves, osteoporosis and other abnormalities (Laurberg *et al.*, 2000). With an aging population, this may become a greater public health concern.

Currently, perchlorate is not regulated in the U.S. under the Federal Safe Drinking Water Act. Occupational health studies at two perchlorate production facilities in the U.S., in which perchlorate exposure was quantified through urinary perchlorate measurements, found no elevation in TSH, drop in  $fT_4$  or other adverse effects (Gibbs *et al.*, 1998). Epidemiological studies on neonatal screening data from California and Nevada health departments showed no increase in incidence of congenital hypothyroidism or decrease in neonatal  $T_4$  associated with perchlorate in drinking water up to 15  $\mu\text{g/L}$  (Lamm and Doemland, 1999; Li *et al.*, 2000). Serum samples were collected from school-age children and newborns in three cities in Chile with reported perchlorate in drinking water (<4, 5 to 7 and 100 to 120  $\mu\text{g/L}$ ). Samples revealed significantly higher free  $T_4$  but normal TSH levels in the two cities with higher perchlorate concentrations (Crump *et al.*, 2000). Dietary iodide in each of the above populations was within normal ranges.

The proposed model describes the kinetics and distribution of perchlorate in the average adult human after exposure to the perchlorate. It also describes iodide kinetics and competitive inhibition of iodide uptake by perchlorate. Perchlorate's transport mechanisms can be modeled similarly to that of iodide, as it binds to the NIS and competitively inhibits iodide uptake (Anbar *et al.*, 1959; Brown-Grant and Pethes, 1959). The kinetics of these anions differ mainly in that iodide is organified in the thyroid (thyroid hormone production) whereas perchlorate is thought to be unreactive and eventually diffuses from the thyroid into systemic circulation. Although perchlorate is quickly eliminated unchanged in the urine (Wolff, 1998), the impact of chronic displacement of iodide from prolonged exposure to perchlorate-contaminated drinking water is the focus of this and ongoing modeling efforts.

The objective of this effort is to simulate serum perchlorate and iodide levels and the subsequent inhibition of iodide uptake into the thyroid. The model does not include effects on thyroid hormone production and homeostasis at this point.

## METHODS

The human data used in model development were obtained from Hays and Solomon (1965) and both published and unpublished data from a recent human study involving drinking water exposure to perchlorate and measured inhibition of radioiodide uptake in the thyroid (Greer *et al.*, 2000).

Data supporting model validation were obtained from another recent but unpublished drinking water study conducted by Drs. Holger Leitolf and Georg Brabant of the Medizinische Hochschule, Hanover, Germany. In addition, urinary perchlorate clearance data by Eichler

(1929), Kamm and Drescher (1973) and Durand (1938) were also used to validate model predictions.

### **Human Iodide Kinetic Data (Hays and Solomon, 1965)**

A comprehensive human kinetic study on early iodide distribution was reported in 1965 by Hays and Solomon. The authors studied the effect of gastrointestinal cycling on iodide kinetics in nine healthy males after an intravenous (*iv*) dose of  $3.44 \times 10^{-3}$  ng  $^{131}\text{I}$ /kg bodyweight. Frequent measurements of radioiodide uptake in the thyroid, gastric secretions, plasma and cumulative urine samples were taken during the three hours following injection. Gastric secretions were collected using a nasogastric tube with constant suction while the subjects remained in a resting position (only standing to urinate). Saliva was not collected separately and therefore pooled, to some extent, with gastric juices. To account for the removal of gastric iodide from circulation and to determine its impact on free iodide distribution, the authors ran a control session on the same subjects without aspirating gastric secretions. Aspirated gastric secretions accounted for 23% of the  $^{131}\text{I}$  administered.

### **Perchlorate Kinetics and Inhibition of Thyroid Iodide Uptake (Greer *et al.*, 2000)**

#### *Perchlorate Data*

Greer *et al.* (2000) recently studied effects on humans of repeated low level exposure to perchlorate. Subjects received 0.5, 0.1, 0.02 or 0.007 mg/kg-day perchlorate in drinking water over a two week period. Each dose group consisted of eight healthy volunteers (four males and four females), with no signs or symptoms of thyroid disorders. The daily dose was dissolved in 400 mL water and divided into four 100 mL servings, which were ingested at approximately 0800, 1200, 1600 and 2000 hours.

Baseline serum and urine samples were collected before the first perchlorate treatment. During perchlorate exposure, serum samples were collected at the following approximate times: day 1 at 1200 and 1600, day 2 at 0800, 1200 and 1700, day 3 at 0900, day 4 at 0800 and 1200, day 8 between 0800 and 0900 and day 14 at 0800 and 1700. Serum samples were also collected on post-exposure days 1, 2, 3 and 14. Twenty-four hour urine collections were taken on exposure days 1, 2, 14 and post-exposure days 1 through 3. Serum and 24 hour urine samples from the study were provided compliments of Dr. Monte Greer of Oregon Health Science University (OHSU), Portland, OR, and Dr. Gay Goodman of Intertox, Seattle, WA; samples were analyzed for perchlorate at the Operational Toxicology Branch, Human Effectiveness Directorate at the Air Force Research Laboratory (AFRL/HEST), Wright Patterson Air Force Base (WPAFB), OH, using the analytical methods described below. A detailed description of the study method is provided in Greer *et al.* (2000).

### *Iodide Inhibition Data*

Eight and 24 hour thyroid  $^{123}\text{I}$  uptakes (radioiodine uptake or RAIU) were measured one to two days prior to perchlorate treatment (baseline), on days 2 and 14 of perchlorate exposure and 14 days after perchlorate. A gelatin capsule containing 100  $\mu\text{Ci}$  of  $^{123}\text{I}$  was administered orally at 0800, before drinking the first perchlorate solution for that day. Thyroid scans were then taken 8 and 24 hours later.

### *Thyroid Hormone Data*

The serum samples were also analyzed for TSH,  $\text{T}_4$ ,  $\text{T}_3$  and  $\text{fT}_4$  at OHSU. These hormone data were not used in the PBPK model described below; however, statistical analysis of the data is described in Attachment 2.

### **Supporting Kinetic Studies**

Both urine and serum perchlorate concentrations were provided from a recent unpublished study by Drs. Brabant and Leitolf of Medizinische Hochschule, Hanover, Germany. In their study, 7 healthy males ingested 12.0 mg/kg-day perchlorate dissolved in 1 liter of drinking water everyday for 2 weeks. The daily perchlorate dose was divided equally in three portions and ingested three times per day (approximately between 0600 and 0800, 1100 and 1300, and 1800 and 2000 hours). Blood specimens were collected on days 1, 7 and 14 of perchlorate treatment and on the two mornings after perchlorate administration was discontinued. Samples were analyzed for perchlorate at AFRL/HEST.

Three published studies reported cumulative urine concentrations collected from healthy males after receiving a high oral dose of perchlorate (Durand, 1938; Kamm and Drescher, 1973; Eichler, 1929). Oral doses administered in these studies were 784 mg  $\text{NaClO}_4$  (635 mg  $\text{ClO}_4^-$ ) (Durand, 1938); 1000 mg  $\text{NaClO}_4$  (765 mg  $\text{ClO}_4^-$ ) (Kamm and Drescher, 1973) and 2000 mg  $\text{KClO}_4$  (1400 mg  $\text{ClO}_4^-$ ) (Eichler, 1929). The studies did not report serum perchlorate levels.

Stanbury and Wyngaarden (1952) measured radioiodide uptake in a patient with Grave's disease. The patient received a tracer dose of  $^{131}\text{I}$  as a control before perchlorate dosing and again one hour after administration of 100 mg  $\text{KClO}_4$ . Thyroid scans of radioiodide uptake were performed both after the control and perchlorate sessions to determine the level of inhibition.

### **Analytical Methods**

Serum samples were analyzed for perchlorate by ion chromatography on a Dionex DX-500 ion chromatography system with a GP-40 gradient pump, CD-20 conductivity detector, a LC-20 chromatography enclosure and an AS40 automated sampler. The injection volume was 200  $\mu\text{L}$ . Anion separation was obtained on a Dionex Ion Pac AS-11, 2.0 x 250-mm separation column

with an AG-11 2.0 x 50 mm guard column and an ATC-1 anion trap column. The mobile phase consisted of 80 mM NaOH. The mobile phase flow rate was set at 0.25 mL/min. Background suppression was achieved by using an Anion Self-Regenerating Suppressor (ASRS)-ULTRA suppressor, with external water flowing at 10 mL/min.

For sample preparation, 50  $\mu$ L of serum was precipitated with 200  $\mu$ L of cold 100% ethanol. Samples were then centrifuged at 14,000 rpm for 30 minutes, using an Eppendorf microcentrifuge. The supernatant was removed and evaporated to dryness under the flow of nitrogen gas. Samples were then reconstituted in 1 mL of 18 M $\Omega$ /cm water. The reconstituted samples were filtered through a Millipore Millex HV-13 0.45 micron syringe filter and placed in 2 mL sample vials for analysis. The samples required no further dilution, making the final dilution after preparation 1:20. To check the performance of the instrument, a duplicate sample, a perchlorate spiked sample and control standards were evaluated after every ten serum samples.

Ion chromatography of urine was performed on a Dionex DX-500 microbore ion chromatograph system with a GP-40 gradient pump, CD-20 conductivity detector, an LC-20 chromatography enclosure and an AS40 automated sampler. The injection volume was 200  $\mu$ L. Anion separation was obtained on a Dionex IonPac AS-11 2.0 x 250-mm separation column with an AG-11 2.0 x 50 mm guard column and an ATC-1 anion trap column. The mobile phase varied from 60 to 120 mM NaOH, depending on the sample. The mobile phase flow rate was set at 0.25 mL/min. Background suppression was achieved by using an Anion Self-Regenerating Suppressor (ASRS)-ULTRA suppressor, with external water flowing at 10 mL/min.

For the sample preparation of urine, 500  $\mu$ L of urine was filtered through a Millipore Millex HV13 0.45 micron syringe filter. The sample was then placed in a Millipore Ultrafree 0.5 centrifuge filter and was centrifuged in an Eppendorf microcentrifuge at 14,000 rpm for 30 minutes. The filtered sample was then removed and diluted 1:500 in 2 mL sample vials. The samples in which no perchlorate was detected were prepared a second time, using the same process as described above, but diluted only 1:50. If there was still no perchlorate detected in the samples, then they again were prepared with the same method as above and diluted 1:25. A 1:25 dilution is the lowest dilution that can be used without producing a significant increase in baseline noise and a subsequent decrease in detection capabilities.

## Model Structure

The human model for perchlorate inhibition of iodide uptake was developed concurrently with the male rat model (Merrill, 2001). Much of the early development was based upon generalizations drawn from in-house work on perchlorate (Fisher *et al.*, 2000) and the work of Hays and Wegner (1965) describing iodide kinetics. Nearly identical model structures were used to describe the kinetics of both iodide and perchlorate, as they share similar ionic size and an affinity for NIS (Figure 1). Tissues, which were reported to have tissue:plasma concentration ratios greater than one and that express NIS were described as compartments of nonlinear saturable uptake. In the model, these tissues include the thyroid, skin and gastric mucosa (Wolff, 1998; Chow *et al.*, 1969; Kotani *et al.*, 1998; Anbar *et al.*, 1959 and Perlman *et al.*, 1941).



Although other tissues have been known to sequester iodide and similar anions (e.g., salivary glands, choroid plexus, ovaries, mammary glands, placenta) (Brown-Grant, 1961; Honour *et al.*, 1952; Spitzweg *et al.*, 1998), the iodide and perchlorate pools of these tissues are expected to be too small to significantly affect plasma levels or were not important in the non-pregnant human. These tissues were therefore lumped with slowly and richly perfused tissues.

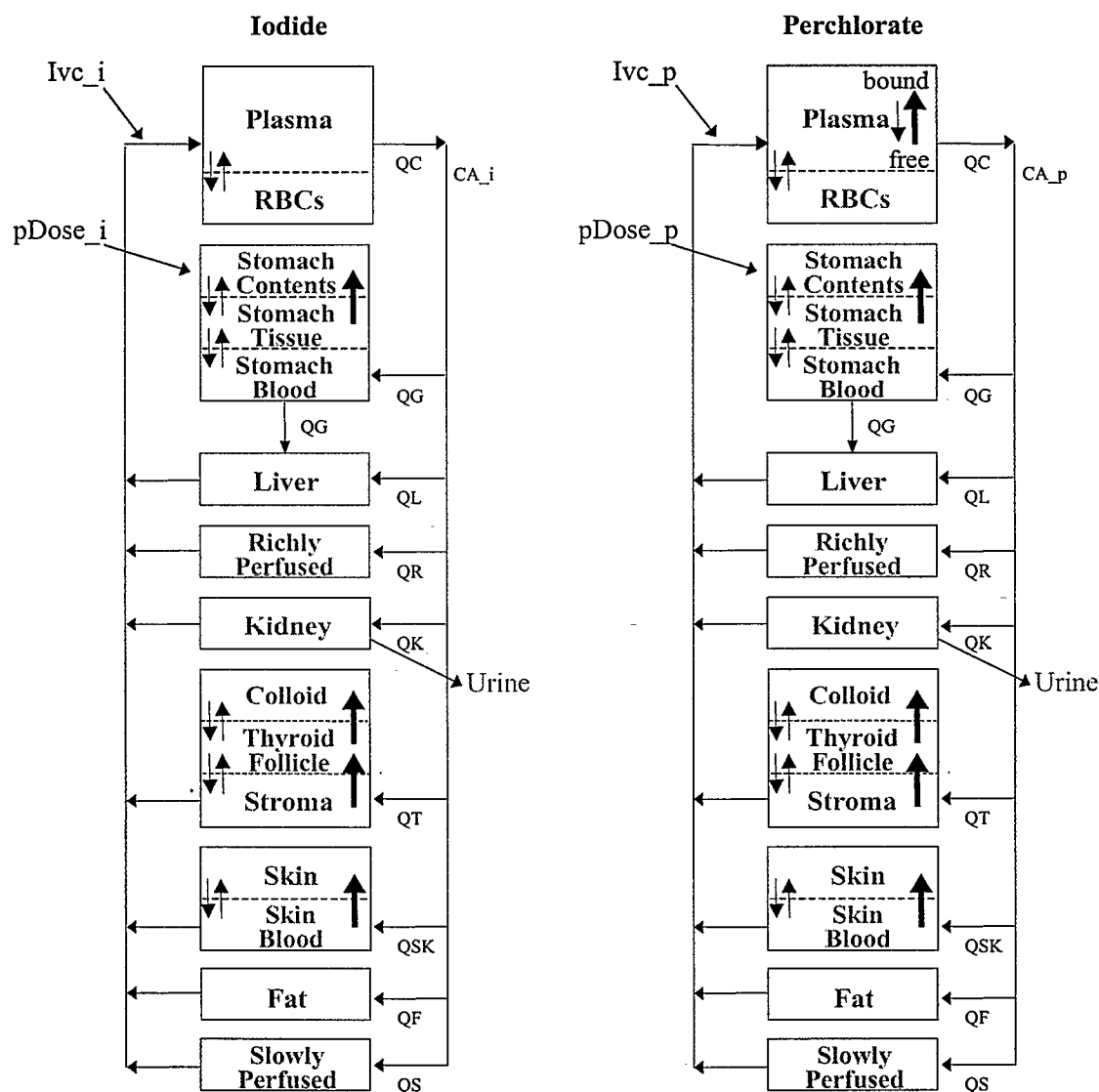


**Figure 1. Schematic of PBPK model for perchlorate and iodide distribution. Bold arrows indicate active uptake at NIS sites (with exception of plasma binding). Small arrows indicate passive diffusion.**

In addition to the thyroid, stomach, skin, slowly and richly perfused compartments, the model also includes separate compartments for plasma, kidney, liver and fat. The kidney was required

to describe urinary clearance of the anions. A liver compartment was maintained separately, as it would be required in future development of the model to include hormone homeostasis. The liver is the primary site of extrathyroidal deiodination. Fat does not absorb either anion well. However, wide variations in percent body fat, between sexes and individuals, in human populations could alter perchlorate/iodide kinetics. Therefore, for the purpose of using the model for species extrapolations, fat is included as an exclusionary compartment.

The stomach and thyroid consist of three sub-compartments representing the stroma, the follicle and the colloid in the thyroid, or the capillary bed, stomach wall and contents in the case of the stomach. The skin contains two sub-compartments representing the capillary bed and the skin tissue. Active uptake into the thyroid colloid, stomach contents and skin were described using Michaelis-Menten kinetics for nonlinear processes (Figure 1, bold arrows). Permeability area cross products (PAs) and partition coefficients (Ps) were used to describe the first order movement of the anions between the capillary bed, tissue and inner compartments (Figure 1, small arrows), which results from the inherent electrochemical gradient within the tissues. Passive diffusion through the kidney, liver and fat compartments were described with partitions and blood flows for these tissues. Plasma binding of perchlorate was described with Michaelis-Menten terms for the association of the  $\text{ClO}_4^-$  anions to plasma binding sites and a first order clearance rate for the dissociation. First order clearance rates from the kidney were also used to describe urinary clearance of the anions.

There are few studies that measured perchlorate or iodide in skin. Yu *et al.* (2000) reported  $^{36}\text{ClO}_4^-$  in male rat skin at higher concentrations than in plasma for several hours after *iv* administration. Zeghal *et al.* (1995) examined the effects of perchlorate on the iodine composition of rat skin. Although Zeghal and his colleagues did not measure skin perchlorate levels directly, they reported a significant reduction in skin iodide in young and adult rats after its administration, suggesting competitive inhibition. Therefore, active uptake was also used to describe the skin compartment for perchlorate.

Iodide has also been reported in the skin at higher concentrations than in plasma after *iv* dosing, but the results have not been consistent. Brown-Grant and Pethes (1959) observed skin:serum ratios as high as 2.0 in adult male rats and 5.0 in young pups. The skin:serum ratio was higher in the adult male than female rats. They did not find skin:serum ratios higher than one in guinea pigs or mice, however. *In vivo* studies with radioiodide in rats resulted in skin:serum iodide ratios near one (Yu *et al.*, 2000), but not at levels as high as those reported by Brown-Grant and Pethes.

This behavior in skin has been reported for another similar anion. Hays and Green (1973) performed dialysis studies on intact human tissues with pertechnetate. They found skin had a relatively slow uptake of pertechnetate peaking at 18 hours and, in fact, more retention after leaching dialysis than brain, muscle and serum.

Clinical scans of radioiodide tracers have not revealed elevated iodide levels in human skin. This does not necessarily imply that iodide is not actively sequestered to some extent in human skin. It is possible that skin radioactivity was diffused enough to be indistinguishable from

background. The fact that NIS expression has been reported in rat skin (Kotani *et al.*, 1998) and the distribution of NIS has been found to be similar across species (Wolff, 1998) suggests that the skin, due to its size, may represent an important pool for slow iodide turnover in humans.

The blood compartment differs between the perchlorate and iodide models. The perchlorate blood compartment is composed of plasma and plasma proteins to simulate binding. Free iodide does not appear to bind to plasma proteins in the same manner as  $\text{ClO}_4^-$  and therefore a single compartment for plasma is used in the iodide model.

### Physiological Parameters

Human tissue volumes and blood flows were obtained from the literature (Table 1). Considerable variability was reported for some parameters. For example, blood flow to the gastrointestinal (GI) tract can increase tenfold in response to enhanced functional activity (secretion and digestion) (Granger *et al.*, 1985). Blood flows used in the model represent estimates of resting values. Human data on the volume of the stomach capillary bed (VGBc) were not found in the published literature. Therefore, a value derived from rat stomach data (Altman and Dittmer, 1971a) was applied as VGBc in the human.

Thyroid volume was obtained from ultrasound measurements on 57 healthy volunteers with no thyroid disorders (37 to 74 years of age), in a study conducted by Yokoyama *et al.* (1986). The mean thyroid volume was  $13.4 \pm 4.1$  mL and mean thyroid volume to bodyweight ratio was  $0.251 \pm 0.074$  mL/kg (mean  $\pm$  standard deviation (s.d.)), approximately 0.03% of bodyweight (BW). They found a positive correlation between thyroid volume and both bodyweight and age, with weight having the most pronounced influence. The percent of total thyroid volume attributed to the thyroid follicular epithelium, colloid and stroma were estimated from histometric measurements of patients at necropsy by Brown *et al.* (1986). Their findings on the histological features of thyroids of men and women showed overlapping distributions without evidence of a significant difference between sexes.

A significant sex difference in total fat mass is reported in humans, with women having approximately 10% more fat than men (Brown *et al.*, 1997). Therefore, a gender-specific value was used for this parameter.

**Table 1. Human physiological parameters**

Physiological Parameters	Human	Source
<b>Tissue Volumes</b>		
Bodyweight BW (Kg)	~70.0	Subject-specific
Slowly Perfused VSc (%BW)	65.1	Brown <i>et al.</i> , 1997
Richly Perfused VRc (%BW)	12.4	Brown <i>et al.</i> , 1997
Fat VFc (%BW)	♂ 21.0 ♀ 32.7	Brown <i>et al.</i> , 1997
Kidney VKc (%BW)	0.44	Brown <i>et al.</i> , 1997
Liver VLc (%BW)	2.6	Brown <i>et al.</i> , 1997
Stomach Tissue VGc (%BW)	1.7	Brown <i>et al.</i> , 1997
Gastric Juice VGJc (%BW)	0.071	Licht and Deen, 1988
Stomach Blood VGBc (%VG)	4.1	Altman & Dittmer, 1971a
Skin Tissue VSkc (%BW)	3.7	Brown <i>et al.</i> , 1997
Skin Blood VSkBc (%VSk)	8.0	Brown <i>et al.</i> , 1997
Thyroid VTtotc (%BW)	0.03	Yokoyama <i>et al.</i> , 1986
Thyroid Follicle VTc (%VTtot)	57.3	Brown <i>et al.</i> , 1986
Thyroid Lumen VDTc (%VTtot)	15.0	Brown <i>et al.</i> , 1986
Thyroid Blood VTBc (%VTtot)	27.6	Brown <i>et al.</i> , 1986
Plasma Vplasc (%BW)	4.4	Marieb, 1992; Altman & Dittmer, 1971b
Red Blood Cells VRBCc (%BW)	3.5	Marieb, 1992; Altman & Dittmer, 1971b
Adjusted Slowly Perfused VS (L)	28.0	Calculated from model
Adjusted Richly Perfused VR (L)	5.34	Calculated from model
<b>Blood Flows</b>		
Cardiac Output QCc (L/hour-kg)	16.5	Brown <i>et al.</i> , 1997; Hanwell & Linzell, 1973
Fat QFc (%QC)	5.2	Brown <i>et al.</i> , 1997
Kidney QKc (%QC)	17.5	Brown <i>et al.</i> , 1997
Liver QLc (%QC)	22.0	Brown <i>et al.</i> , 1997
Stomach QGc (%QC)	1.0	Leggett & Williams, 1995; Malik <i>et al.</i> , 1976
Thyroid QTc (%QC)	1.6	Brown <i>et al.</i> , 1997
Adjusted Slowly Perfused QS (%QC)	13.0	Calculated, using 24% QC as flow to all slowly perfused tissues (Brown <i>et al.</i> , 1997)
Adjusted Richly Perfused QR (%QC)	33.0	Calculated, using 76% QC as flow to all richly perfused tissues (Brown <i>et al.</i> , 1997)

### Partitioning Coefficients

Partition coefficients for iodide and perchlorate were estimated from *in vivo* studies (Table 2). Tissue and serum measurements from steady state conditions were not available. Therefore, they were estimated from the clearance portion of the data collected after acute dosing. Halmi *et al.* (1956) measured organ to serum concentration ratios for radioiodide in rats approximately 1, 4 and 24 hours after an *iv* dose of the tracer iodide. The average liver:serum and muscle:serum iodide ratios at approximately 4 hour after an injection of  $^{131}\text{I}$  (0.40 and 0.21, respectively) were used to represent human rapidly and slowly perfused partitioning coefficients for iodide.

Perlman *et al.* (1941) reported similar iodine ratios in rabbit tissues five hours after subcutaneous dosing with NaCl and a tracer amount of iodide (0.44 for liver/blood and 0.19 for muscle/blood). These liver:blood and muscle:blood, ratios reported by Perlman remained relatively constant for up to 96 hours.

Perchlorate partition coefficients for rapidly (0.56) and slowly perfused (0.31) tissues were derived from in-house rat studies, 24 hours after a single *iv* dose of 3.3 mg  $^{36}\text{ClO}_4^-/\text{kg}$  (Yu *et al.*, 2000). Anbar *et al.* (1959) reported similar liver:blood and muscle:blood ratios of 0.38 and 0.12, respectively, in rabbits 12 hours after an intraperitoneal dose of 100 mg  $\text{KClO}_4$ .

A value of 0.05 was reported for the partitioning of perchlorate into the fat of a hen (Pena *et al.*, 1976). This value was also used to represent iodide partitioning into fat in our model, since other tissue:serum concentration ratios from Pena's hen study were consistent with ratios found in both the rat (Yu *et al.*, 2000) and rabbit (Anbar *et al.*, 1959).

For compartments with nonlinear uptake of the anions, effective partition coefficients were used, representing either approximate tissue:serum concentration ratios or electrical potential gradients. The effective partition coefficients for iodide in the stomach compartments were also derived from in-house rat experiments. Stomach wall:serum and gastric juice:stomach wall perchlorate ratios of 1.8 and 2.3, respectively, were derived 24 hours after the *iv* dose. Estimated stomach iodide partitions, derived from in-house  $^{125}\text{I}$  kinetic studies, were 1.0 for the stomach tissue:serum and 3.5 for the gastric juice:stomach ratios (Yu, 2000).

Skin measurements from the in-house  $^{36}\text{ClO}_4^-$  kinetic study were highly variable and suggested an effective partitioning greater than one. Based on the 24 hour timepoint, an effective partition coefficient of 1.15 was derived (Yu, 2000). The iodide value used (0.7) was derived from Perlman *et al.* (1941). They reported skin:plasma iodide ratios from 0.6 to 0.7 in rabbits, 6 to 96 hours after a subcutaneous dose of tracer radioiodide. This is in agreement with in-house  $^{125}\text{I}$  studies, which suggest a partition coefficient less than 1.0 (Yu *et al.*, 2000).

Chow and Woodbury (1970) measured electrochemical potentials within the thyroid stroma, follicular membrane and colloid at three different doses of  $\text{ClO}_4^-$ . Their measured difference in electrical potential between the thyroid stroma and follicle can be interpreted as an effective partition coefficient for charged moieties, such as  $\text{ClO}_4^-$  and  $\text{I}^-$ , hindering the entry of negatively charged ions into the follicle. The equal and opposite potential from the follicle to the colloid enhances passage of negatively charged species into the colloid and indicates an effective partition coefficient of greater than one.

From Chow and Woodbury (1970), the potential difference for the stroma:follicle interface ranges from  $-58$  to  $-51$  mV, from which an effective partitioning between 0.114 and 0.149 is calculated (Clewell, 2001a; Merrill, 2001). Similarly, the follicle:lumen potential ranges from  $+50$  to  $+58$  mV, resulting in an effective partition between 6.48 and 8.74. These values were also used to describe the uptake of iodide based on the fact that iodide and perchlorate have the same ionic charge (-1) and similar ionic radii and therefore react similarly to the electrochemical gradient.

**Table 2. Chemical specific parameters for human model**

Partition Coefficients (unitless) Ps	Iodide	Perchlorate	Source
Slowly Perfused / Plasma PS	0.21	0.31	Halmi <i>et al.</i> , 1956; Yu <i>et al.</i> , 2000
Richly Perfused / Plasma PR	0.40	0.56	Halmi <i>et al.</i> , 1956; Yu <i>et al.</i> , 2000
Fat/ Plasma PF	0.05	0.05	Pena <i>et al.</i> , 1976
Kidney/ Plasma PK	1.09	0.99	Perlman <i>et al.</i> , 1941; Yu <i>et al.</i> , 2000
Liver/Plasma PL	0.44	0.56	Perlman <i>et al.</i> , 1941; Yu <i>et al.</i> , 2000
Gastric Tissue/Gastric Blood PG	0.50	1.80	Yu <i>et al.</i> , 2000; Yu, 2000
Gastric Juice/Gastric Tissue PGJ	3.50	2.30	Yu <i>et al.</i> , 2000; Yu, 2000
Skin Tissue/Skin Blood PSk	0.70	1.15	Perlman <i>et al.</i> , 1941; Yu, 2000
Thyroid Tissue/Thyroid Blood PT	0.15	0.13	Chow & Woodbury (1970)
Thyroid Lumen/Thyroid Tissue PDT	7.00	7.00	Chow & Woodbury (1970)
Red Blood Cells/Plasma	1.00	0.80	Rall <i>et al.</i> , 1950; Yu <i>et al.</i> , 2000
<b>Max Capacity, Vmaxc's (ng/hr-kg)</b>			
Thyroid Colloid Vmaxc DT	1.0E+8	2.5E+5	Fitted
Thyroid Follicle Vmaxc T	~1.5E+5	5.0E+4	Fitted
Skin Vmaxc S	7.0E+5	1.0E+6	Fitted
Gut Vmaxc G	9.0E+5	1.0E+5	Fitted
Plasma binding Vmaxc Bp	---	5.0E+2	Fitted
<b>Affinity Constants, Km's (ng/L)</b>			
Thyroid Lumen Km DT	1.0E+9	1.0E+8	Golstein <i>et al.</i> , 1992
Thyroid Km T	4.0E+6	1.8E+5	Gluzman & Niepomnischcz, 1983; Wolff, 1998
Skin Km S	4.0E+6	2.0E+5	Gluzman & Niepomnischcz, 1983; Wolff, 1998
Gut Km G	4.0E+6	2.0E+5	Gluzman & Niepomnischcz, 1983; Wolff, 1998
Plasma binding Km B	---	1.8E+4	Fitted
<b>Permeability Area Cross Products, PAs (L/hr-kg)</b>			
Gastric Blood to Gastric Tissue PAGc	0.2	0.6	Fitted
Gastric Tissue to Gastric Juice PAGJc	2.0	0.8	Fitted
Skin Blood to Skin Tissue PASKc	0.06	1.0	Fitted
Plasma to Red Blood Cells PARBCc	1.0	1.0	Fitted
Follicle to Thyroid blood PATc	1.0E-4	1.0E-4	Fitted
Lumen to Thyroid Follicle PADTc	1.0E-4	0.01	Fitted
<b>Clearance Values, Cl's (L/hr-kg)</b>			
Urinary excretion CLUc	0.1	0.126	Fitted
Plasma unbinding Clunbc	---	0.025	Fitted

**Note:** All parameters listed are notated in the model by either an *i* (for iodide) or *p* (for perchlorate) following the parameter name (e.g., PR<sub>i</sub>, PR<sub>p</sub>, Vmaxc<sub>Ti</sub>, Vmaxc<sub>Tp</sub>, etc.)

### Affinity Constants and Maximum Velocities

Gluzman and Niepomnischcz (1983) derived a mean Michaelis-Menten affinity constant (Km) of  $4.0 \times 10^6$  ng/L for iodide from thyroid slices of 5 normal individuals. The thyroid slices were incubated with several medium iodide concentrations. The authors noted little variation between normal and pathological human thyroid specimens, or between thyroid specimens of different

species. Therefore, a  $K_m$  value of  $4.0 \times 10^6$  ng/L was assumed to describe the uptake of iodide in compartments involving active uptake by NIS (thyroid and gastric juices).

Wolff (1998) noted that iodide's  $K_m$  for NIS is similar in different tissues. Wolff also noted that the  $K_m$  for perchlorate and other similar monovalent anions decreased with the anions' ability to inhibit iodide uptake. Several studies suggest perchlorate is a more potent inhibitor than iodide. In the rat thyroid, Wyngaarden *et al.* (1952) have shown that perchlorate was a more powerful inhibitor of the iodide trap than thiocyanate. Halmi and Stuelke (1959) showed that perchlorate was ten times as effective as iodide in depressing tissue to blood ratios in the rat thyroid and gut. Similarly, Harden *et al.* (1968) compared human saliva to plasma radioiodide concentration ratios after equimolar doses of perchlorate and iodide. The saliva/plasma iodide ratios, during resting conditions, were approximately seven times lower after a molar equivalent dose of perchlorate vs. iodide. Lazarus *et al.* (1974) also demonstrated that perchlorate was taken up to greater extent in mice salivary glands than iodide. Based on this information, a  $K_m$  between  $1.8 \times 10^5$  and  $2.0 \times 10^5$  ng/L, approximately 10 times lower than that of iodide, was estimated to represent perchlorate's higher affinity for NIS.

The apical follicular membrane also exhibits a selective iodide uptake mechanism. Golstein *et al.* (1992) found the  $K_m$  for iodide transport from the bovine thyroid follicle into the colloid ( $K_m\_DTp$ ) to be approximately  $4.0 \times 10^9$  ng/L. This iodide channel also appears to be very sensitive to perchlorate inhibition. The ability of perchlorate to inhibit iodide uptake at the apical follicular membrane suggests that the  $K_m$  of perchlorate at the apical follicular membrane ( $K_m\_Dtp$ ) is also lower than that of iodide. Model simulations of thyroid inhibition supported a value of  $1.0 \times 10^8$  ng/L, approximately ten times less than that of iodide for this channel also.

Whereas the  $K_m$  is similar across tissues containing NIS, the maximum velocity term ( $V_{max}$ ) does vary between tissues and species (Wolff, 1998), being lower in humans than other species (Gluzman and Niepomnische, 1983; Wolff and Maurey, 1961) when expressed per gram of tissue. Maximum velocities or capacities ( $V_{maxc}$ ) were not found in the literature and were therefore estimated for a given compartment by fitting the simulation to the data at varying doses (Table 2).

TSH increases the total amount of NIS in a membrane, thereby increasing the thyroid  $V_{max}$ . Gluzman and Niepomnische (1983) measured elevated  $V_{max}(s)$  in thyroid specimens from subjects with Grave's disease, toxic adenoma and dishormonogenetic goiter. In specimens from non-toxic nodular goiter, Hashimoto's thyroid or extranodular tissue from toxic adenoma, maximum capacities were decreased. They found no significant difference between normal human glands and warm nodules from nodular goiters. In addition to hyper- or hypo-stimulation of trapping activity (thyroid disorders), the intrathyroidal iodide pool and the magnitude of iodide efflux are also responsible for variations in  $V_{max}$  (Bagchi and Fawcett, 1973). Currently the iodide model does not account for TSH stimulation and endogenous iodide pools.

TSH regulation is reported to be unique to the thyroid NIS and does not regulate uptake in other tissues with NIS (Cavaliere, 1997). Spitzweg *et al.* (2000) suggest the up-regulation of NIS protein expression in mammary glands of lactating rats may be regulated by prolactin and/or

oxytocin (Spitzweg *et al.*, 2000), inferring that other agents may stimulate NIS expression and function. The effect of TSH on iodide transport may also be physiologically responsive to other hormones and growth factors. Most growth factors are reported to decrease the ability of TSH to stimulate iodide accumulation, with the exception of insulin, which has an opposite effect (Carrasco, 1993).

### Fitting Model Parameters to Experimental Data

Parameter terminology used in this model is summarized in Table 2. Simultaneous differential equations, which simulate radioiodide and perchlorate distribution in the proposed mathematical model, were written and solved using ACSL™ (Advanced Continuous Simulation Language) software (AEgis Technologies, Austin, TX).

### Permeability Area Cross Products and Clearance Values

Diffusion limited uptake in tissues requiring subcompartments (e.g., the stomach, thyroid and skin) were described using permeability area cross products (PA) (L/hour·kg) and partition coefficients (P). The PA values in this model were fitted by setting the partition coefficients to the literature values in Table 2. The equations below illustrate the use of PAs:

$$RAXB\_y = QX \times (CA\_y - CVXB\_y) + PAX\_y \times \left( \frac{CX\_y}{PX\_y} - CVXB\_y \right)$$

$$AXB\_y = \int_0^t (RAXB\_y) dt$$

$$CVXB\_y = AXB\_y / VXB$$

$$RAX\_y = PAX\_y \times \left( CVXB\_y - \frac{CX\_y}{PX\_y} \right)$$

$$AX\_y = \int_0^t (RAX\_y) dt$$

$$CX = AX / VX$$

where:

$RAXB\_y$	=	Net rate of uptake of $y^{th}$ anion ( $I^-$ or $ClO_4^-$ ) into $X^{th}$ tissue's capillary bed (ng/hour)
$AXB\_y$	=	Amount of $y^{th}$ anion in $X^{th}$ tissue's capillary bed (ng)
$QX$	=	Blood flow through $X^{th}$ tissue (L/hour)
$CA\_y$	=	Arterial blood concentration of $y^{th}$ anion (ng/L)
$RAX\_y$	=	Net rate of uptake of $y^{th}$ anion into $X^{th}$ tissue (ng/hour)
$AX\_y$	=	Amount of $y^{th}$ anion in $X^{th}$ tissue (ng)
$CVXB\_y$	=	Venous blood concentration of $y^{th}$ anion (ng/L)
$CX\_y$	=	Tissue concentration of $y^{th}$ anion (ng/L)



Fitted clearance values were used to describe first order urinary excretion rates and reversible plasma binding to serum, as shown below:

$$RAX\_y = CX\_y \times CLX\_y$$

where:  $RAX$  = rate of clearance of  $y^{th}$  anion from  $X^{th}$  compartment (ng/hour)  
 $CX\_y$  = concentration of  $y^{th}$  anion within  $X^{th}$  compartment (ng/L)  
 $CLX\_y$  = clearance value of  $y^{th}$  anion into  $X^{th}$  compartment (L/hour)

### Saturable Processes

The basic equation used to simulate active uptake of iodide and perchlorate alone (without accounting for inhibition) in tissues with NIS activity is:

$$\frac{dAX\_y}{dt} = \frac{Vmax\_Xy \times CVX\_y}{Km\_Xy + CVX\_y}$$

where:

$AX\_y$  = Amount of  $y^{th}$  anion in  $X^{th}$  tissue (ng)  
 $t$  = Time (hour)  
 $Vmax\_Xy$  = Maximum uptake of  $y^{th}$  anion at  $X^{th}$  tissue's symporter (ng/hour)  
 $Km\_Xy$  = Michaelis-Menten (M-M) affinity constant for  $y^{th}$  anion in  $X^{th}$  compartment (ng/L)  
 $CVX\_y$  = Concentration of  $y^{th}$  anion in capillary blood of  $X^{th}$  compartment (ng/L)

Accounting for inhibition of active uptake of either iodide or perchlorate in the presence of the competing anion is expressed as:

$$\frac{dAX\_y}{dt} = \frac{Vmax\_Xy \times CVX\_y}{Km\_Xy \times \left(1 + \frac{CVX\_z}{Km\_Xz}\right) + CVX\_y}$$

where:

$Km\_Xz$  = M-M affinity constant for  $z^{th}$  anion (competitive inhibitor) in  $X^{th}$  compartment (ng/L)  
 $CVX\_y$  = Concentration of  $z^{th}$  anion (competitive inhibitor) in venous capillary blood of  $X^{th}$  compartment (ng/L)

Example equations for simulating the transport of iodide ( $i$ ) through the thyroid ( $T$ ) are provided below. The equations include blood flow through the thyroid capillary bed (stroma) as well as active uptake and inhibition by perchlorate in both the follicle and colloid. The transport of the anions through other tissues of active uptake is similar.

- Rate of change in thyroid blood ( $RATB_i$ )

$$RATB_i = QT \times (CA_i - CVTB_i) + PAT_i \times \left( \frac{CT_i}{PT_i} - CVTB_i \right) - RupT_i$$

- Rate of change in follicle ( $RAT_i$ )

$$RAT_i = RupT_i + PAT_i \times \left( \frac{CVTB_i - CT_i}{PT_i} \right) - RupDT_i + PADT_i \times \left( \frac{CDT_i}{PDT_i} - CT_i \right)$$

- Rate of change in Colloid ( $RADT_i$ )

$$RADT_i = RupDT_i + PADT_i \times \left( \frac{CT_i - CDT_i}{PDT_i} \right)$$

- Rate of active uptake in the follicle ( $RupT_i$ ) with inhibition by perchlorate ( $_p$ )

$$RupT_i = \frac{V_{max\_Ti} \times CVTB_i}{Km\_Ti \times \left( 1 + \frac{CVTB_i}{Km\_Tp} \right) + CVTB_i}$$

- Rate of active uptake into the colloid ( $RupDT_i$ ) with inhibition by perchlorate ( $_p$ )

$$RupDT_i = \frac{V_{max\_DTi} \times CT_i}{Km\_DTi \times \left( 1 + \frac{CT_i}{Km\_DTP} \right) + CT_i}$$

## Allometric Scaling

To account for parameter differences due to varying bodyweights of rats and humans, allometric scaling was applied to maximum velocities ( $V_{max}$ ), PAs, clearance values (Cl), tissue volumes (V) and blood flows (Q). The scaling equations are provided in Merrill, 2000.

## RESULTS AND DISCUSSION

### Parameterization of Iodide Model

Development of the iodide model was performed by fitting the model to  $^{131}\text{I}$  kinetic data from Hays and Solomon (1965).  $K_m$ s and partition coefficients were available from literature and/or derived by fitting the model to in-house time course data measured in the male rat, as described earlier.  $V_{max}$  values and PAs were derived by fitting the model simulations to radioiodide ( $^{131}\text{I}$ ) uptake in the thyroid and gastric juice, as described in the following paragraphs. The urinary clearance value was derived by fitting model simulations of cumulative iodide in urine to the observed measurements.

In the 1965 study by Hays and Solomon, aspirated gastric juice accounted for an average of 23% of the *iv* dose within 3 hours of the injection. These data were used to develop the rate of  $^{131}\text{I}$  transfer in and out of gastric juice. Simulation of the gastric juice removed during the aspiration session (Figure 2C) required mathematically removing the amount of  $^{131}\text{I}$  reabsorbed by the stomach wall. This was accomplished by adjusting the rate of reabsorption of  $^{131}\text{I}$  from gastric juice to gastric tissue during the aspiration session. Therefore the term  $RAGJ\_i$  (the rate of change in  $^{131}\text{I}$  in the gastric juice), as it is used in the calculation of  $RAG\_i$  (the rate of change in  $^{131}\text{I}$  in the gastric tissue), described below, is adjusted as follows:

$$RAG\_i = PAG\_i \times \left( \frac{CVGB\_i - CG\_i}{PG\_i} \right) + RAGJ\_i - RupGJ\_i$$

where:

$RupGJ\_i$  = the rate of active uptake of  $^{131}\text{I}$  at the symporter and secretion into gastric juice and  $RAGJ\_i$  is calculated under normal conditions (control session) as:

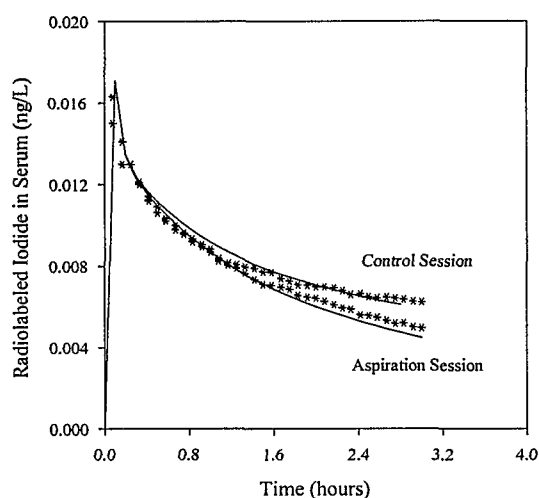
$$RAGJ\_i = PAGJ\_i \times \left( \frac{CGJ\_i}{PGJ\_i - CG\_i} \right) + RupGJ\_i$$

To remove the secreted  $^{131}\text{I}$  in gastric juice from recirculation during the aspiration session, the above equation is modified to eliminate the partitioning of  $^{131}\text{I}$  from gastric juice back into systemic circulation as shown below:

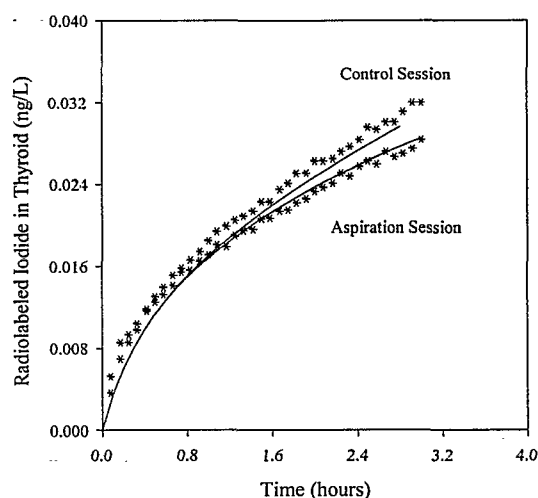
$$RAGJ\_i = PAGJ\_i * (-CG\_i) + RupGJ\_i$$

The  $V_{max}$ 's for the stomach and thyroid were then obtained by fitting values of  $^{131}\text{I}$  uptake into gastric juice from the aspiration session (lower lines in Figures 2B and C).  $PAGJc\_i$ , representing  $^{131}\text{I}$  transfer from the gastric juice into the gastrointestinal plasma was fit to the curve of total  $^{131}\text{I}$  in the aspirated gastric secretions (Figure 2C). The urinary clearance value ( $Cluc\_i$ ) was fitted to simulate both cumulative urine content and plasma iodide from the aspiration session data (lower lines in Figures 2A and D).

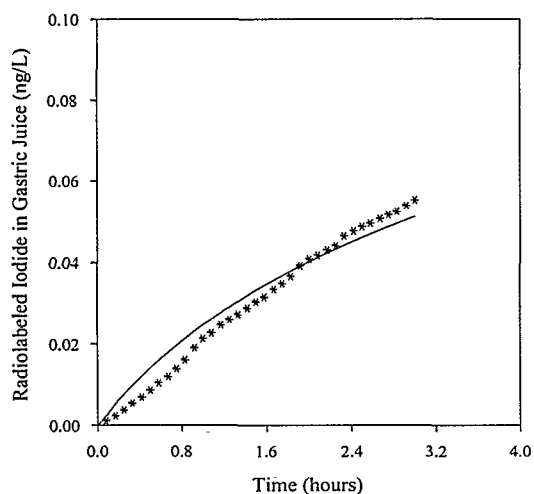
Once parameters were established using the aspiration session,  $PAG\_i$  was fitted to predict the corresponding increase in  $^{131}\text{I}$  in plasma, thyroid and urine seen in the control session versus the aspiration session. (upper lines in Figures 2A, B and D).



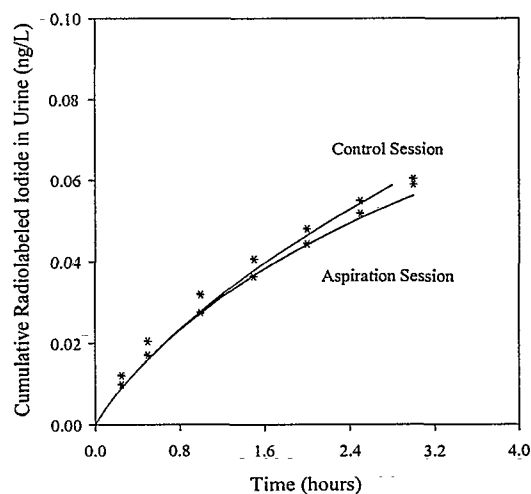
A



B



C

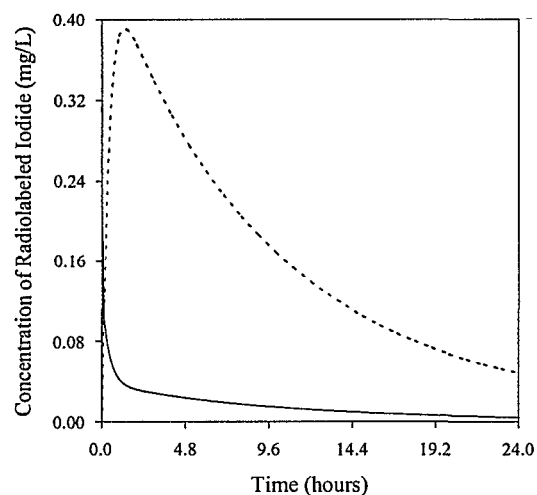


D

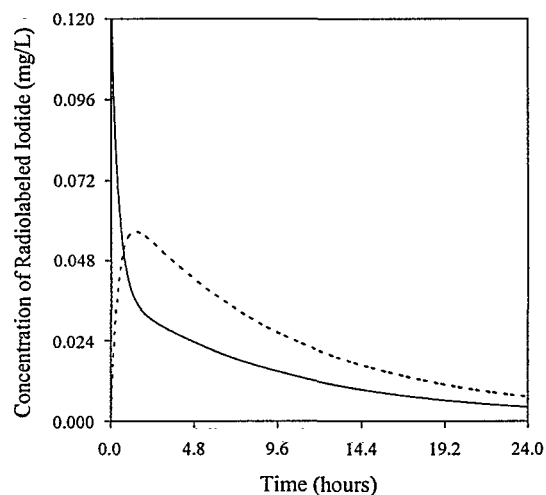
**Figure 2. Mean  $^{131}\text{I}$  in plasma (A), thyroid (B), gastric juice (C) and urine (D) of nine healthy males after an *iv* dose of  $10\ \mu\text{Ci } ^{131}\text{I}$  ( $\sim 3.44\ \text{ng/kg}$ ) (Hays and Solomon, 1965). Model predicted (lines) and actual values (stars) are presented for both the control and aspiration sessions.**

Kinetic data on radioiodide or perchlorate uptake in human skin were not available. Effective partitions, described above, were estimated from literature (Table 2). A saturable skin compartment was required in order to fit the human serum  $^{131}\text{I}$  concentrations in Figure 2. In addition, the trend of the simulated human skin concentrations was compared to the trend seen in the male rat time course data (see corresponding male rat model in Merrill (2000)). In the male rat, skin  $^{125}\text{I}$  concentrations plateau approximately 2.3 times higher than serum concentrations within 4 hour after injection.  $^{125}\text{I}$  appears to diffuse slowly out of skin. Therefore, after

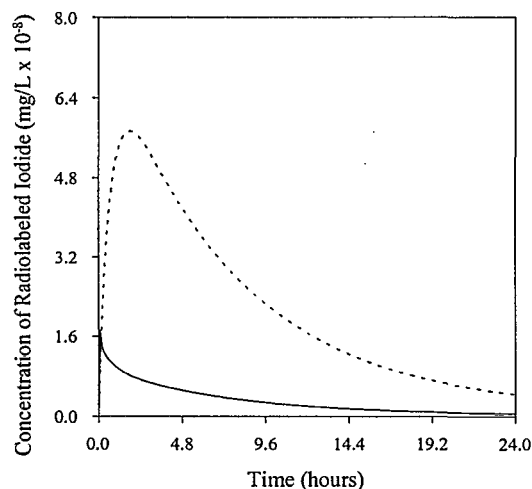
Vmaxc\_S and PASKc values were adjusted to achieve serum fits, the simulated relationship between skin and serum iodide concentrations were compared with those of the male rat (Figure 3 B and D).



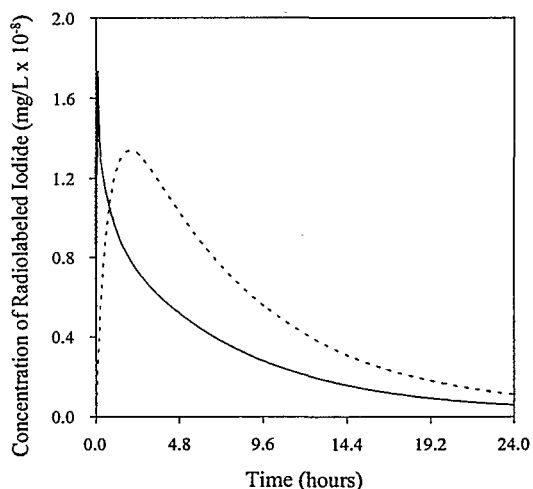
A. Simulations of stomach contents versus serum in the male rat



B. Simulations of skin versus serum in the male rat



C. Simulations of stomach contents versus serum in the human



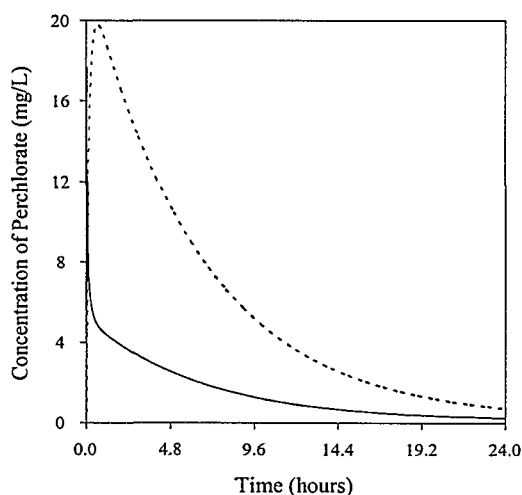
D. Simulations of skin versus serum in the human

**Figure 3. Comparison of model simulations of  $^{131}\text{I}$  concentrations in stomach contents (dotted line) and skin (dashed line) in relation to plasma  $^{131}\text{I}$  concentration (solid line) in the male rat (A and B) and the human (C and D). Corresponding doses between the male rat and human are not shown. The simulations in the male rat (A and B) represent actual fits from an *iv* dose of  $0.033 \text{ mg/kg } ^{125}\text{I}$  taken from Merrill (2000). In the human simulations (C), plasma and stomach contents are actual fits from an *iv* dose of  $3.44 \text{ ng/kg } ^{131}\text{I}$  (see Figures 2 A and C), while the skin simulation (D) is hypothetical.**

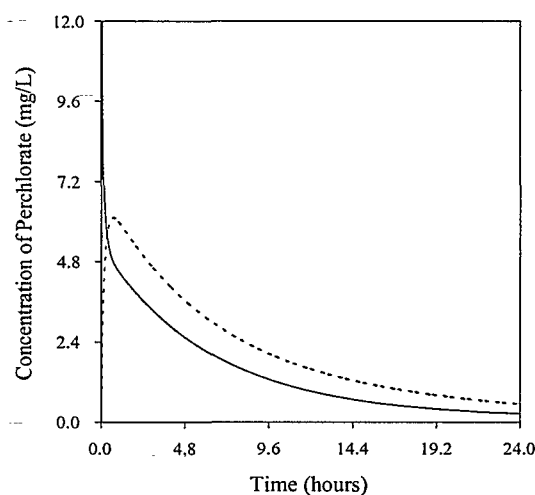
## Parameterization of the Perchlorate Model

As with the iodide model, partitions and  $K_m$  values were derived from the literature and in-house studies, leaving  $V_{max}$  values and PAs to be derived from model fitting. Kinetic perchlorate data in humans were limited to serum and urine concentrations. Therefore, predicted perchlorate levels in human stomach contents, skin and thyroid are hypothetical. The fitting of the iodide model described above resulted in parameters similar to those of the male rat (Merrill, 2000) with the exception of the  $V_{maxc}$  values of the thyroid follicular epithelium and colloid. Based on this comparison, it was assumed that perchlorate parameters in the human would also share similar values to those fitted for the rat.

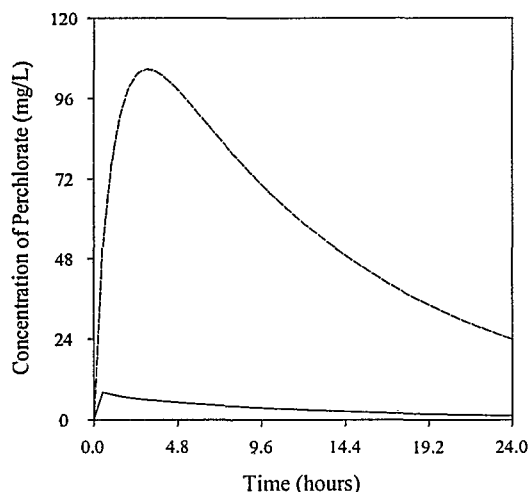
PAs and  $V_{max}$  values of the stomach and skin were adjusted to simultaneously simulate serum perchlorate concentrations and cumulative perchlorate excreted in urine, established by adjusting the urinary clearance value ( $CIU_p$ ). Resulting trends of the predicted human stomach and skin levels over time were then compared to the same trends in the male rat and found to be similar (Figure 4 A-D).



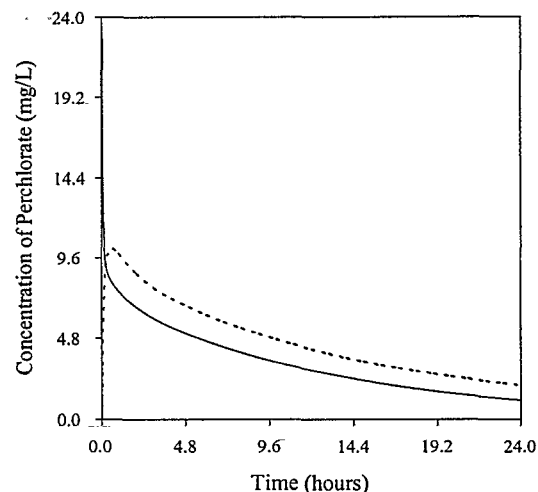
A. Simulated stomach contents (dotted lines) and serum (solid line) in male rat



B. Simulated skin (dotted lines) and serum (solid line) in male rat



C. Simulated stomach contents (dashed lines) and serum (solid line) in human



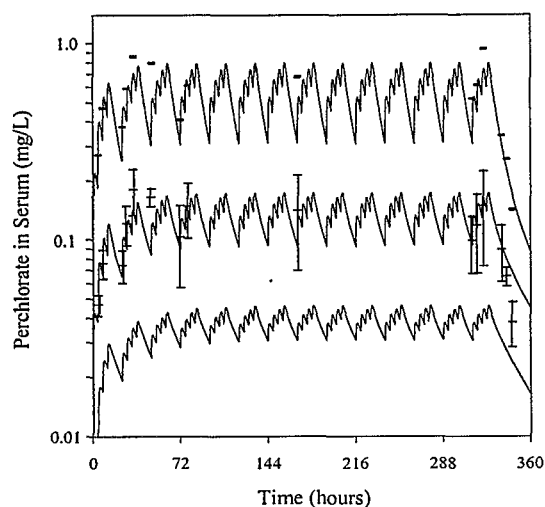
D. Simulated skin (dashed lines) and serum (solid line) in human

**Figure 4. Comparison of model simulations of  $\text{ClO}_4^-$  concentration in stomach contents and skin (dotted line) in relation to plasma  $\text{ClO}_4^-$  concentration (solid line) in the male rat (A and B) and human (C and D) after an *iv* dose of 3 mg/kg  $\text{ClO}_4^-$ . Rat simulations (A and B) are based on actual fits of data taken from Merrill (2001). Human simulations (C and D) are hypothetical fits.**

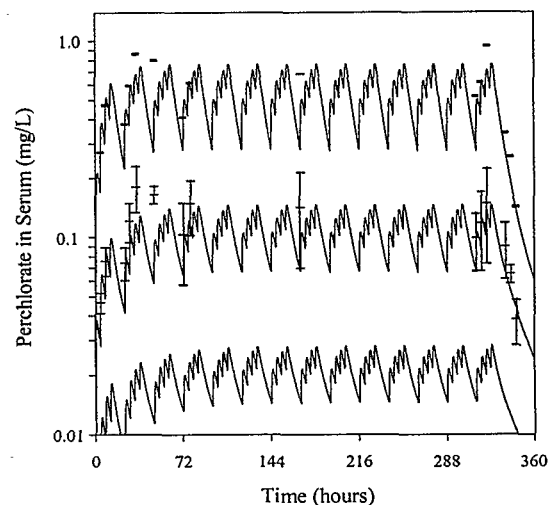
### Plasma Protein Binding

Early model simulations at 0.1 mg/kg-day underestimated serum perchlorate concentrations while still fitting urinary excretion of  $\text{ClO}_4^-$  (Figure 5A and 6). The low serum predictions suggested either less uptake into other tissues or plasma protein binding. Because serum concentrations in the 0.5 mg/kg-day dose group were fitted using the same parameters, plasma protein binding appeared to be the most likely hypothesis. Increasing uptake in other tissues such as skin and gut resulted in the underestimation of serum levels at 0.5 mg/kg-day. In addition, literature studies suggest perchlorate binding in human serum (Scatchard and Black, 1949; Hays and Green, 1973). Plasma binding was modeled to successfully achieve fits of model simulations to serum  $\text{ClO}_4^-$  data at the 0.5, 0.1 and 0.02 dose groups with a common set of parameters (Figure 5B). The model indicates that humans have a lower binding capacity for  $\text{ClO}_4^-$  than rats. For example the  $V_{\text{maxc}}$  for  $\text{ClO}_4^-$  is  $9.3 \times 10^3$  ng/hour-kg in the male rat versus  $5.0 \times 10^2$  ng/hour-kg in the human.

The literature suggests that the hypothesized binding site for perchlorate is albumin. A discussion of these studies is provided in Merrill (2001). The difference between adding plasma binding and not is subtle at 0.5 mg/kg-day; however binding does improve uptake and clearance fits in the 0.1 and 0.02 mg/kg-day groups.



A  
A



B

**Figure 5. Model simulations (lines) with plasma binding (A) and without (B) and means and standard deviations in the observed values (cross bars) from 4 male subjects dosed 0.02, 0.1 and 0.5 mg/kg-day for 14 days (Greer *et al.*, 2000).**

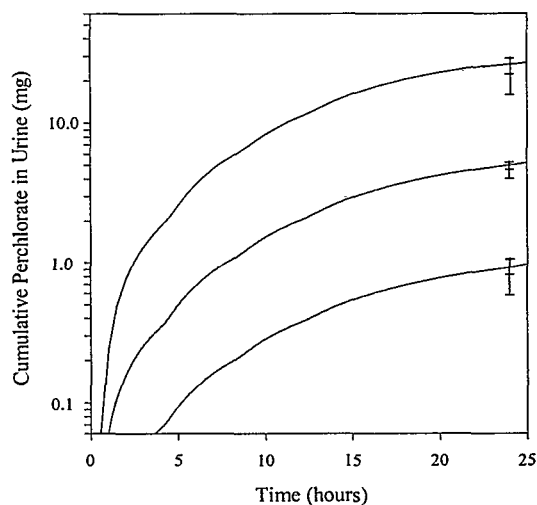
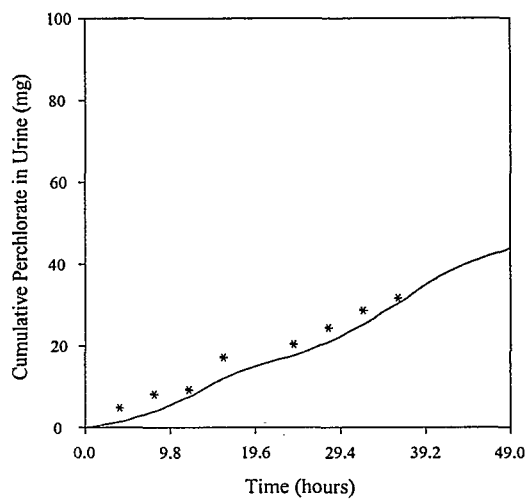
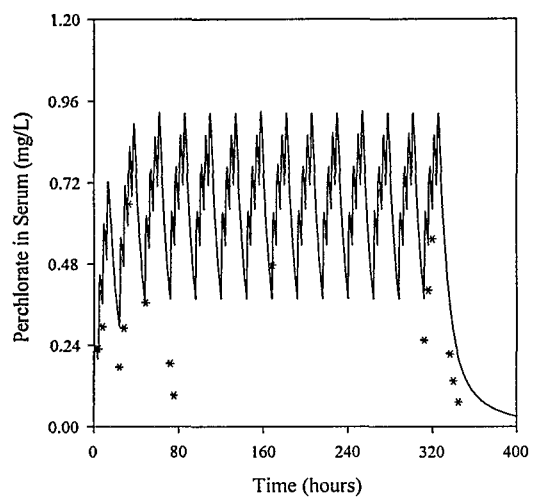


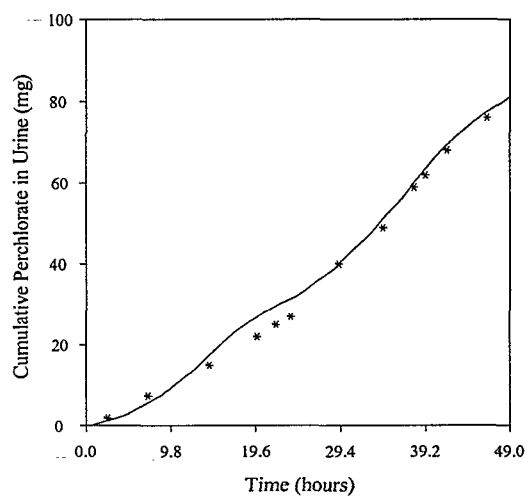
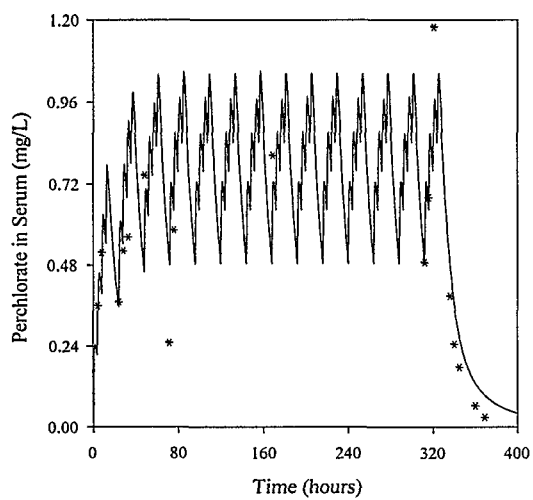
**Figure 6. Model simulations (lines) and mean and standard deviations of the observed cumulative urine (cross bars) in male subjects dosed 0.02, 0.1 and 0.5 mg/kg-day (Greer *et al.*, 2000)**

Serum and cumulative urine perchlorate levels were simulated for each individual in the 0.5, 0.1 and 0.02 mg/kg-day dose groups. An average value for urinary clearance of perchlorate,  $Cl_{Uc\_p}$ , of 0.126 L/hour-kg ( $\pm 0.050$ ) was calculated from the individually fitted values. The following plots show the fit obtained for several subjects obtained by using the average value for  $Cl_{Uc\_p}$  (Figures 7 through 9).

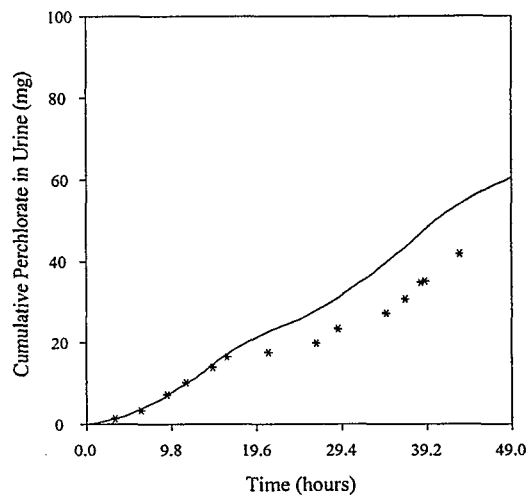
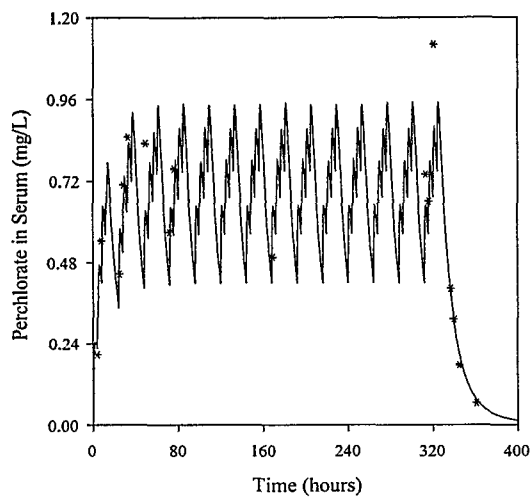




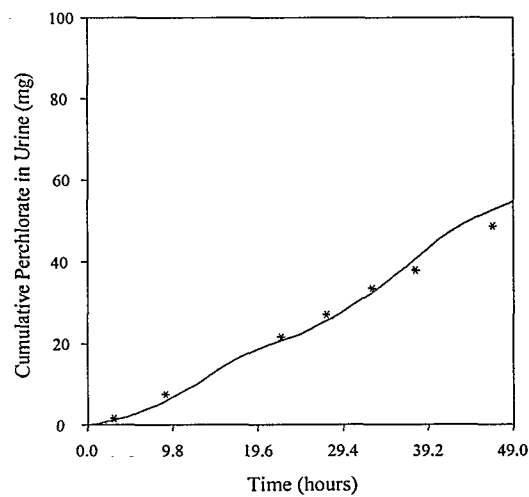
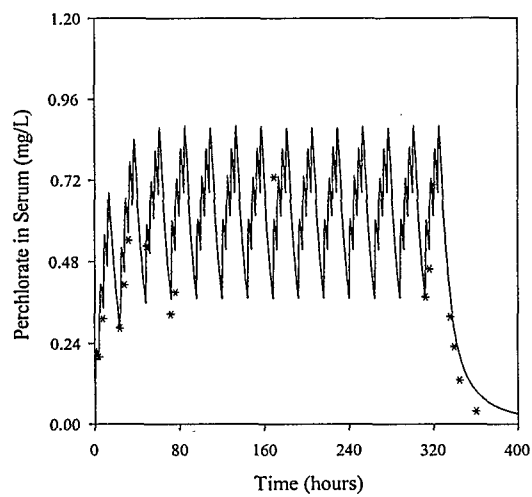
**A**



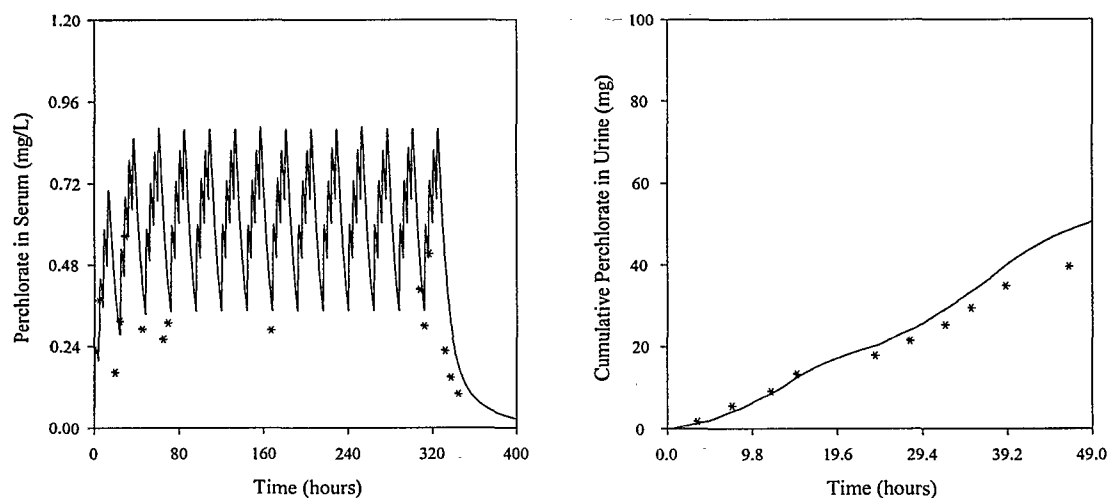
**B**



C

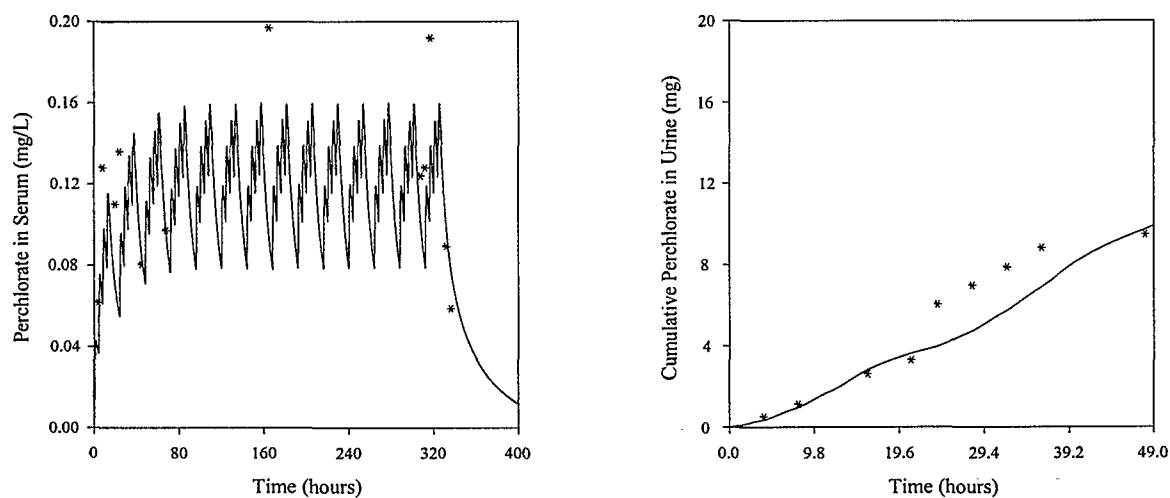


D

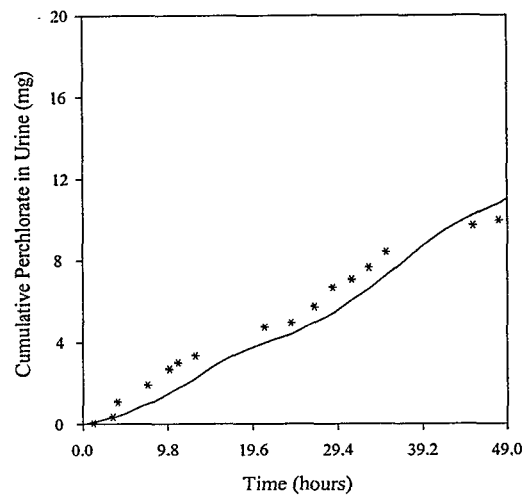
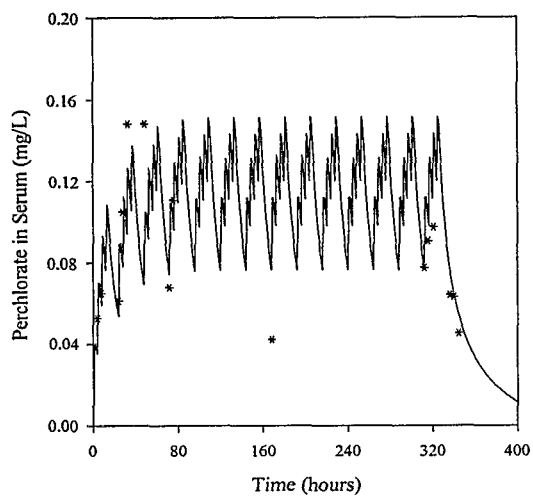


E

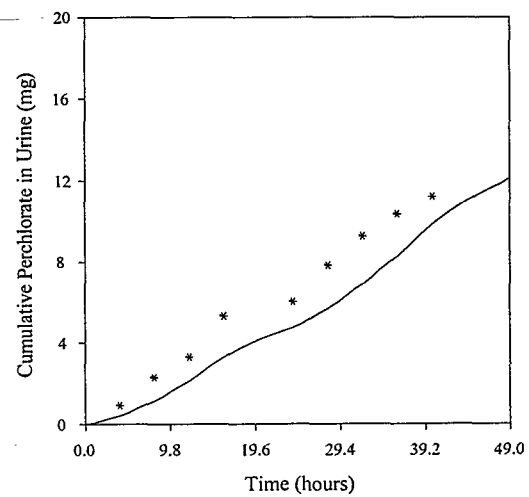
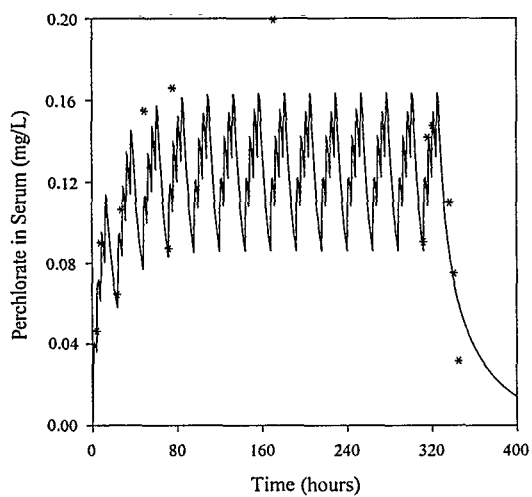
**Figure 7. Model predicted (lines) and actual values (asterisks) of individuals' serum perchlorate concentrations and their corresponding 48 hour cumulative urine perchlorate amounts from 4 healthy subjects who consumed 0.5 mg/kg-day perchlorate in drinking water, 4 times per day for 14 days. Model predictions obtained by using the average value for CIUc<sub>p</sub> (Greer *et al.*, 2000).**



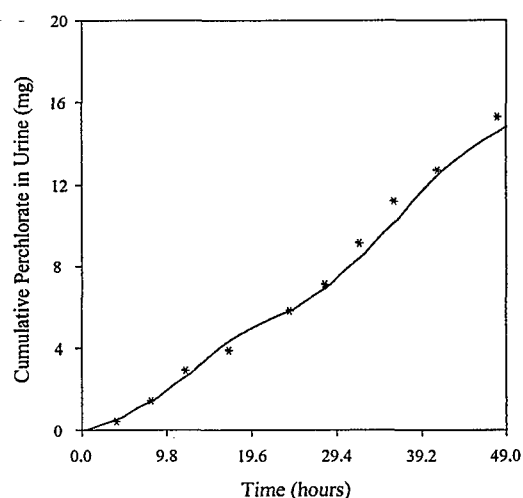
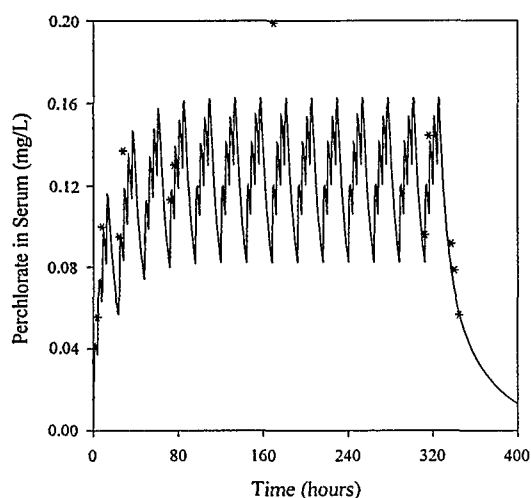
A



**B**



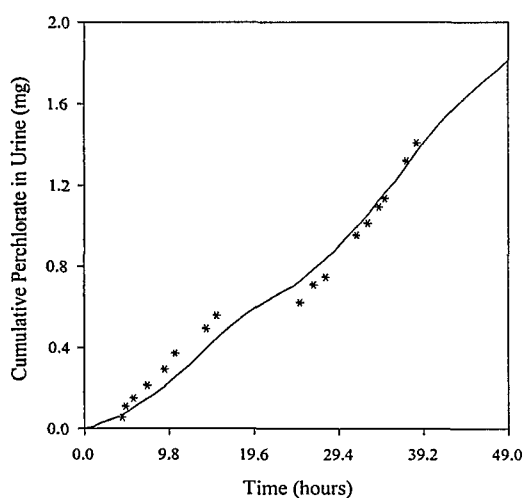
**C**



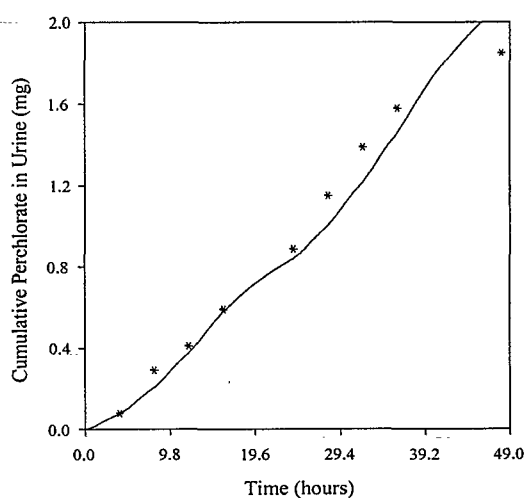
D

**Figure 8. Model predicted (lines) and actual values (asterisks) of individuals' serum perchlorate concentrations and their corresponding 48-hour cumulative urine perchlorate from 4 healthy subjects who consumed 0.1 mg/kg-day perchlorate in drinking water 4 times per day for 14 days. Model predictions obtained by using an average CIUc\_p (Greer *et al.*, 2000).**

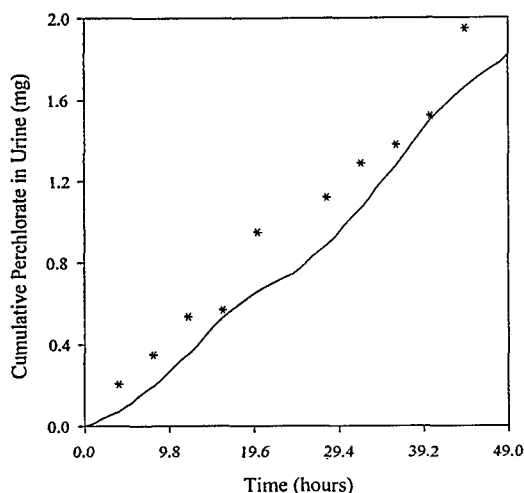
Serum perchlorate levels were not available for the 0.02 mg/kg-day dose group; however, cumulative urine values were fitted (Figure 9) using the average CIUc\_p (0.126 L/hour-kg) calculated from the individual fits in the 0.1 and 0.5 mg/kg-day dose groups.



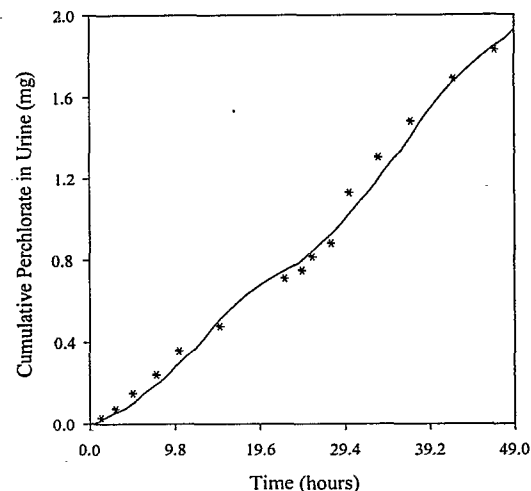
A



B



C



D

**Figure 9. Model simulations (lines) and experimental data (asterisks) of cumulative perchlorate in urine over 48 hours from 4 healthy subjects who consumed 0.02 mg/kg-day perchlorate in drinking water. Model predictions obtained by using the average  $Cl_{UC\_p}$  (Greer *et al.*, 2000).**

### Perchlorate Induced Inhibition of Thyroid Iodide Uptake

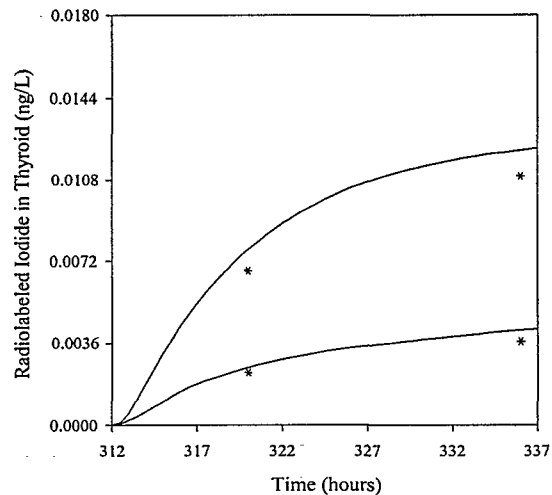
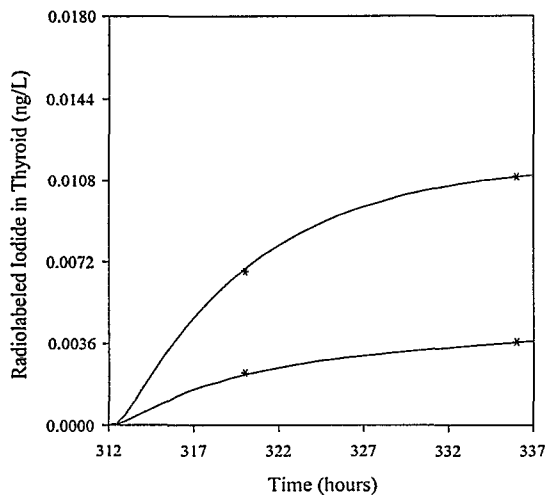
Due to its small size, variations in the thyroid parameters have little effect on serum concentrations of both iodide and perchlorate. As described previously, iodide parameters, including those of the thyroid, were estimated from fits of the data from Hays and Solomon (1965) (see Table 2 and Figure 2B). Using the same iodide parameters, baseline thyroid radioiodide uptakes were fitted by adjusting the  $V_{max}$  for the follicular epithelium ( $V_{maxc\_Ti}$ ) (Figures 10 through 14). An average  $V_{maxc\_Ti}$  ( $1.5 \times 10^5$  ng/hour-kg) was obtained from fitting baseline radioiodide uptake measurements provided by Greer *et al.* (2000) across doses (see Table 3). The large variability in  $V_{maxc\_Ti}$ , ranging from  $5.0 \times 10^4$  to  $5.0 \times 10^5$  ng/hour-kg, may be attributed to variability in endogenous iodide levels, as dietary iodide was not controlled. All participants in each dose group were healthy and screened for thyroid disorders.

Thyroid parameters for perchlorate were assumed to be similar to those of the male rat, with exception of the  $V_{max}$  value in the follicular epithelium and colloid ( $V_{maxc\_Tp}$  and  $V_{maxc\_DTp}$ , respectively), which were increased approximately by the same proportional increase in  $V_{maxc\_Ti}$  and  $V_{maxc\_Dti}$  from the male rat to the human (established by fitting the thyroid radioiodide data by Hays and Solomon (1965)). Table 3 summarizes the individually fit urinary clearance constants for perchlorate and  $V_{maxc\_Ti}$  uptake resulting from each subject in the Greer *et al.* (2000) study.

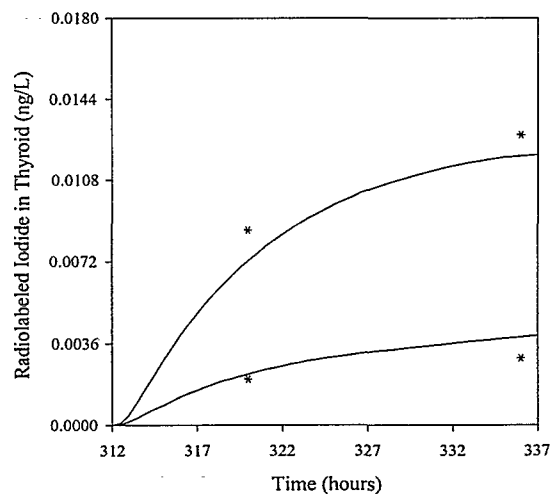
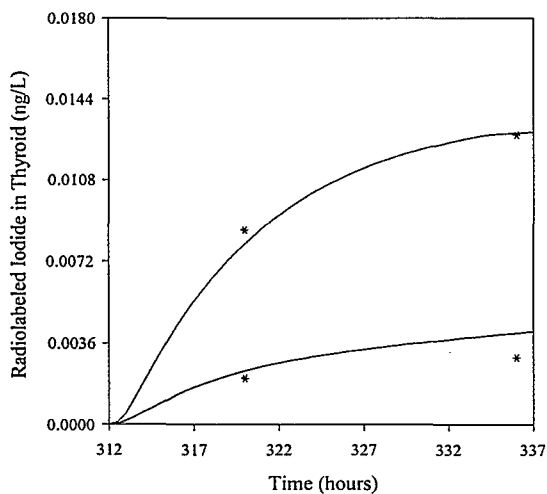
**Table 3. Individually fitted CIUc\_p(s) and Vmaxc\_Ti(s) (Greer *et al.*, 2000)**

<b>Dose Group</b>	<b>Subject</b>	<b>Sex</b>	<b>CIUc_p (L/hr-kg)</b>	<b>Vmaxc_Ti (ng/hr/kg)</b>
0.5 mg/kg/d	AN	f	0.10	1.34E+05
	DR	m	0.09	1.20E+05
	JS1	m	0.10	2.00E+05
	CW	f	0.09	1.80E+05
	TO	m	0.09	2.50E+05
	MA	m	0.09	8.00E+04
	AB1	f	0.10	5.00E+05
	RC	f	0.10	1.00E+05
Group Mean			0.10	1.96E+05
Group Std Dev			0.01	1.35E+05
0.1 mg/kg/d	RT	f	0.10	1.10E+05
	NR	m	0.20	2.20E+05
	KN	m	0.20	6.80E+04
	JF	f	0.12	1.50E+05
	RB1	m	0.24	1.20E+05
	AH	f	0.10	1.60E+05
	SG	f	0.13	5.00E+04
	AB2	m	0.17	1.20E+05
Group Mean			0.16	1.25E+05
Group Std Dev			0.05	5.35E+04
0.02 mg/kg/d	SV	f	NA	1.50E+05
	CB	f	0.10	1.40E+05
	QY	m	0.15	8.00E+04
	DH	m	*	1.50E+05
	JS2	m	NA	1.40E+05
	SK	f	0.20	1.50E+05
	DC	f	0.11	9.00E+04
	GB	m	0.06	8.00E+04
Group Mean			0.12	1.23E+05
Group Std Dev			0.05	3.28E+04
0.007 mg/kg/d	RB	f	NA	1.35E+05
	PE	m	NA	1.35E+05
	MJ	f	NA	7.80E+04
	SE	f	NA	8.00E+04
	EA	f	NA	1.40E+05
	LB	f	NA	2.80E+05
	LR	f	NA	9.00E+04
Group Mean			NA	1.34E+05
Group Std Dev			NA	6.99E+04
<b>Total Mean</b>			<b>0.13</b>	<b>1.45E+05</b>
<b>Total Std Dev</b>			<b>0.05</b>	<b>8.17E+04</b>

**Note:** The 0.007 mg/kg-day dose was run to obtain inhibition data only. Serum and urine samples were not collected.

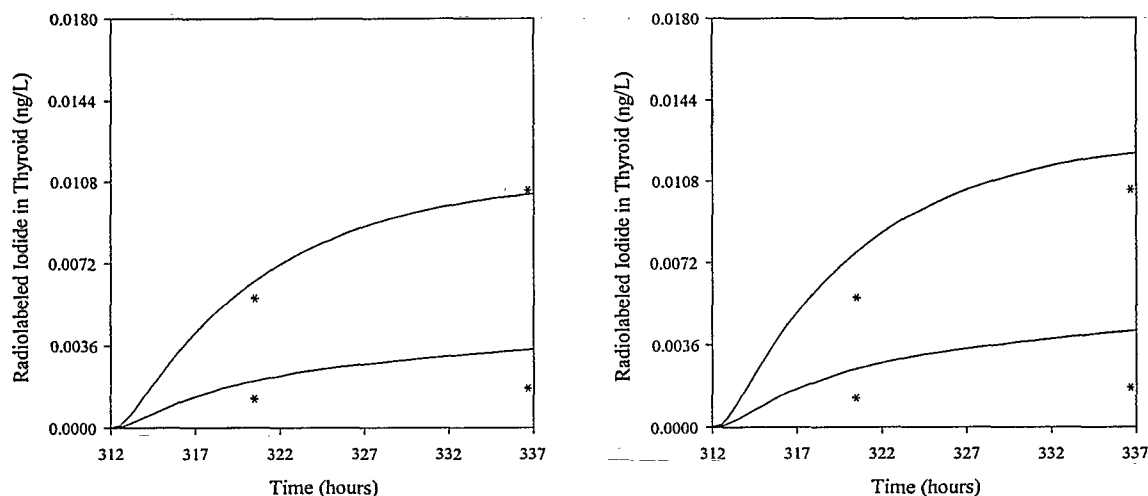


**A.** Thyroid radioiodide uptakes (before perchlorate) (top asterisks) and on day 14 of perchlorate exposure at 0.5 mg/kg-day (bottom asterisks) in a healthy female. Simulation on left obtained by using individually fitted  $V_{maxc\_Ti}$  of  $1.3 \times 10^5$ . Right simulation obtained using average  $V_{maxc\_Ti}$ .

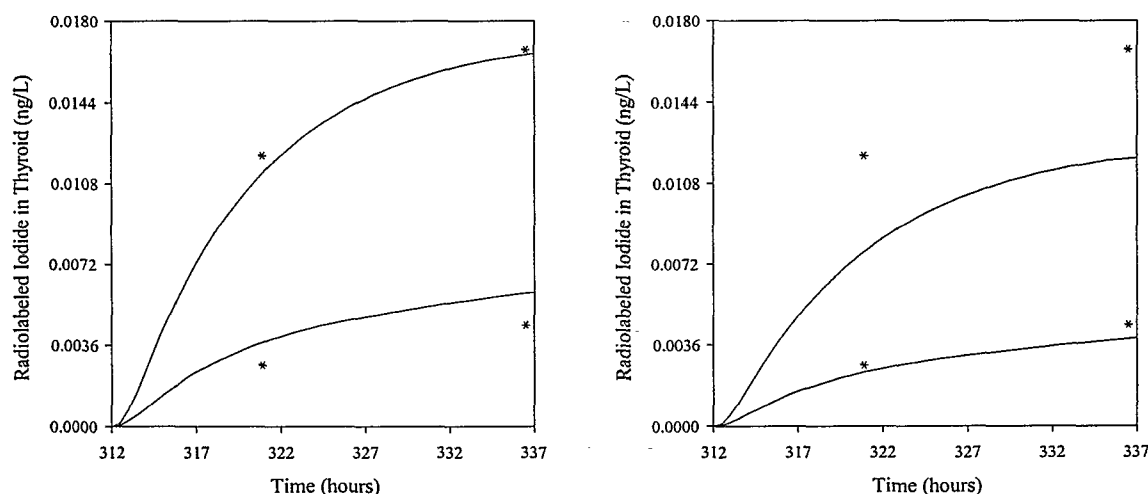


**B.** Thyroid radioiodide uptakes (before perchlorate) (top asterisks) and on day 14 of perchlorate exposure at 0.5 mg/kg-day (bottom asterisks) in a healthy female. Simulation on left obtained by using individually fitted  $V_{maxc\_Ti}$  of  $1.8 \times 10^5$ . Right simulation obtained using average  $V_{maxc\_Ti}$ .



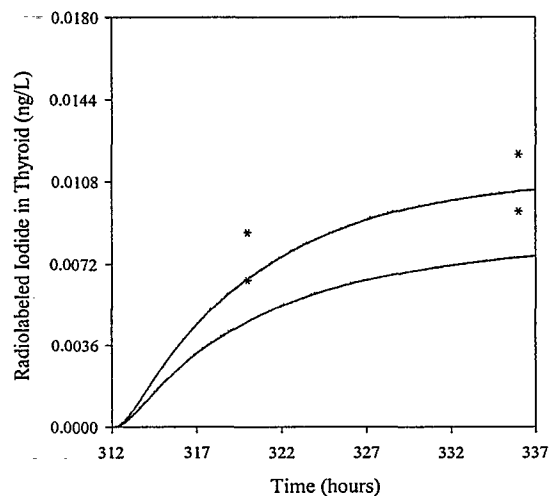
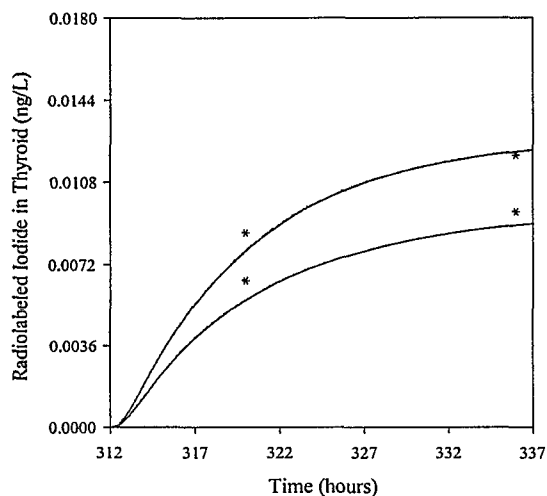


C. Thyroid radioiodide uptakes (before perchlorate) (top asterisks) and on day 14 of perchlorate exposure at 0.5 mg/kg-day (bottom asterisks) in a healthy male. Simulation on left obtained by using individually fitted  $V_{maxc\_Ti}$  of  $1.24 \times 10^5$ . Right simulation obtained using average  $V_{maxc\_Ti}$ .

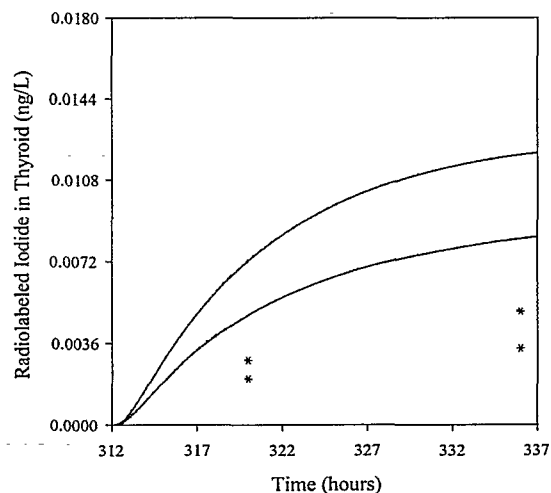
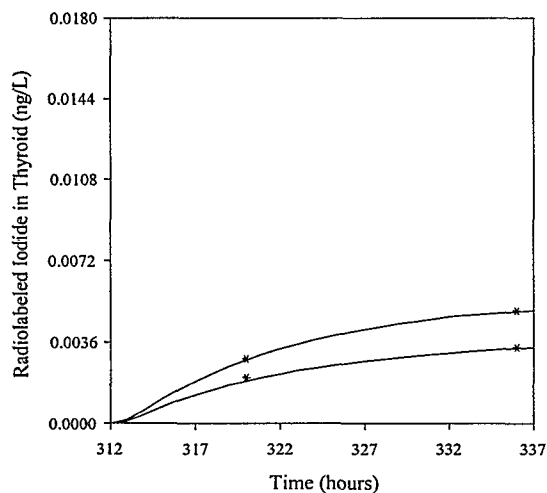


D. Thyroid radioiodide uptakes (before perchlorate) (top asterisks) and on day 14 of perchlorate exposure at 0.5 mg/kg-day (bottom asterisks) in a healthy male. Simulation on left obtained by using individually fitted  $V_{maxc\_Ti}$  of  $2.5 \times 10^5$ . Right simulation obtained using average  $V_{maxc\_Ti}$ .

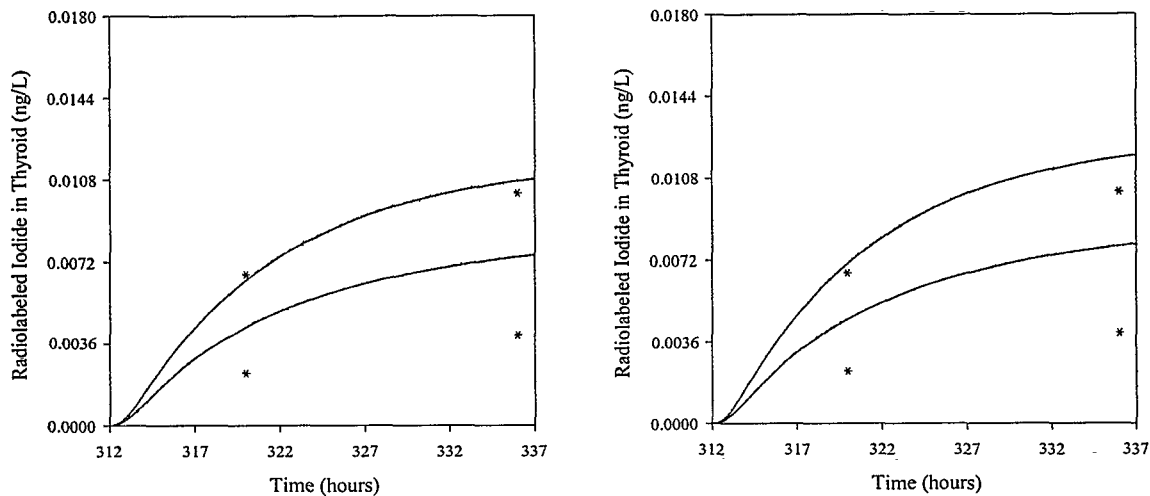
**Figure 10. Model predicted (lines) and actual 8 and 24 hour RAIU measurements (asterisks) from 4 healthy subjects before perchlorate exposure (upper lines and asterisks) and on day 14 of perchlorate exposure at 0.5 mg/kg-day (lower lines and asterisks). Simulations in the figures on the right represent individual fits of thyroid iodide uptake by adjusting  $V_{maxc\_Ti}$ . Simulations in the left figures were established by using the average  $V_{maxc\_Ti}$  (Greer *et al.*, 2000).**



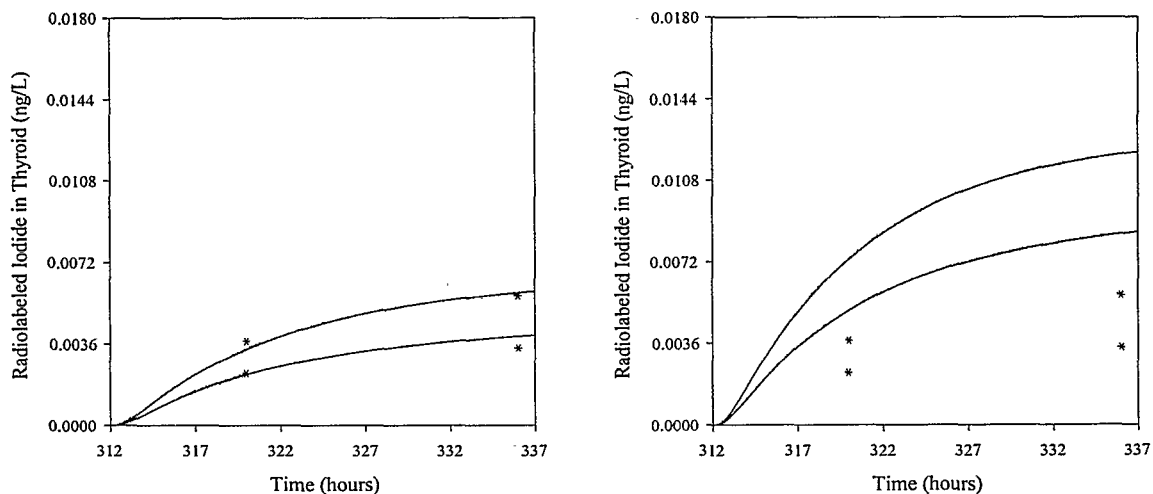
**A.** Thyroid radioiodide uptakes (before perchlorate) (top asterisks) and on day 14 of perchlorate exposure at 0.1 mg/kg-day (bottom asterisks) in a healthy female. Simulation on the left obtained by using individually fitted  $V_{maxc\_Ti}$  of  $1.65 \times 10^5$ . Right simulation obtained using average  $V_{maxc\_Ti}$ .



**B.** Thyroid radioiodide uptakes (before perchlorate) (top asterisks) and on day 14 of perchlorate exposure at 0.1 mg/kg-day (bottom asterisks) in a healthy female. Simulation on the left obtained by using individually fitted  $V_{maxc\_Ti}$  of  $5.0 \times 10^4$ . Right simulation obtained using average  $V_{maxc\_Ti}$ .

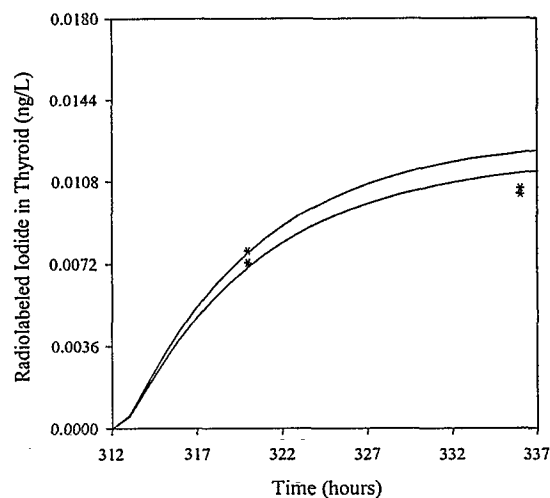
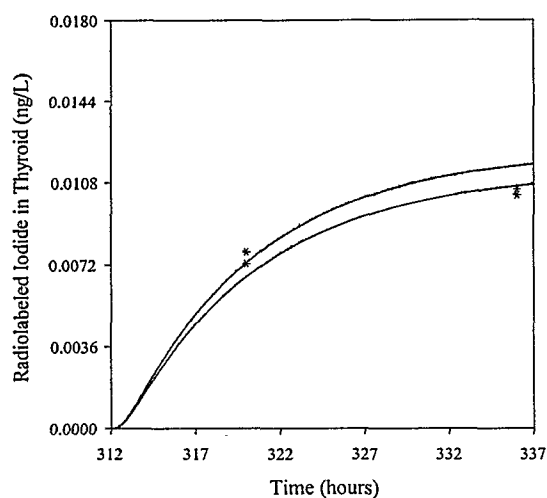


C. Thyroid radioiodide uptakes (before perchlorate) (top asterisks) and on day 14 of perchlorate exposure at 0.1 mg/kg-day (bottom asterisks) in a healthy male. Simulation on the left obtained by using individually fitted  $V_{maxc\_Ti}$  of  $1.2 \times 10^5$ . Right simulation obtained using average  $V_{maxc\_Ti}$ .

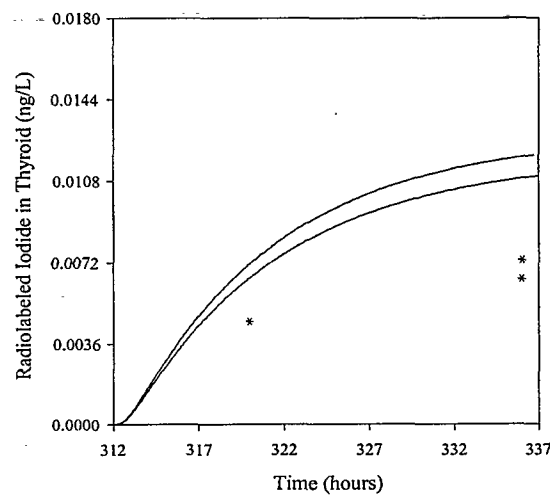
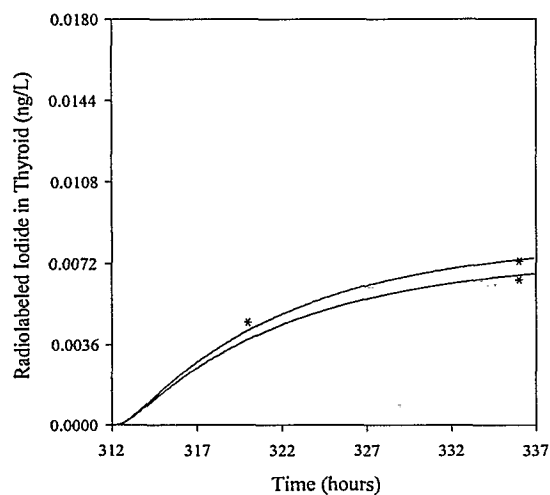


D. Thyroid radioiodide uptakes (before perchlorate) (top asterisks) and on day 14 of perchlorate exposure at 0.1 mg/kg-day (bottom asterisks) in a healthy male. Simulation on the left obtained by using individually fitted  $V_{maxc\_Ti}$  of  $6.8 \times 10^4$ . Right simulation obtained using average  $V_{maxc\_Ti}$ .

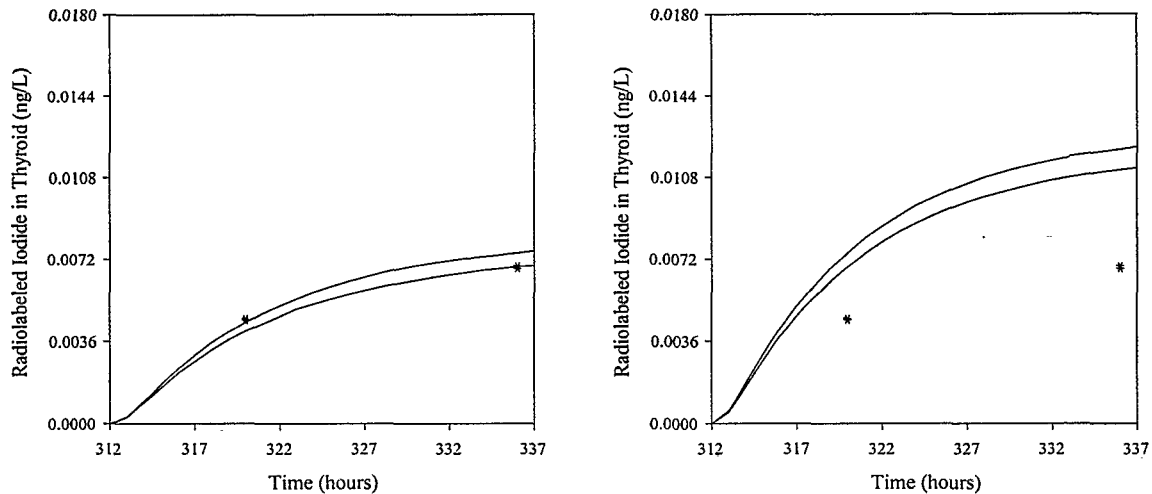
**Figure 11. Model predicted (lines) and observed 8 and 24 hour RAIU measurements (asterisks) during baseline (upper lines and asterisks) and on day 14 of perchlorate exposure at 0.1 mg/kg-day (lower lines and asterisks) from 4 healthy subjects. Simulations on the left were obtained by individual fits of thyroid radioiodide uptakes by adjusting  $V_{maxc\_Ti}$ . Simulations on the right were obtained by using an average  $V_{maxc\_Ti}$  of 150,000 ng/hour-kg (Greer *et al.*, 2000).**



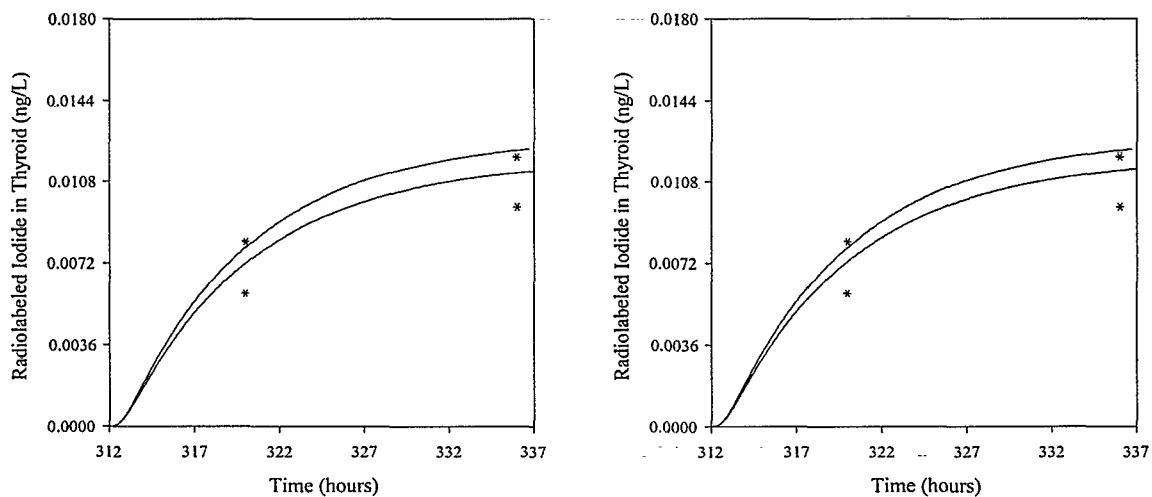
**A.** Thyroid radioiodide uptakes (before perchlorate) (top asterisks) and on day 14 of perchlorate exposure at 0.007 mg/kg-day (bottom asterisks) in a healthy female. Simulation on the left obtained by using individually fitted  $V_{maxc\_Ti}$  of  $1.4 \times 10^5$ . Right simulation obtained using average  $V_{maxc\_Ti}$ .



**B.** Thyroid radioiodide uptakes (before perchlorate) (top asterisks) and on day 14 of perchlorate exposure at 0.02 mg/kg-day (bottom asterisks) in a healthy male. Simulation on the left obtained by using individually fitted  $V_{maxc\_Ti}$  of  $8.0 \times 10^4$ . Right simulation obtained using average  $V_{maxc\_Ti}$ .

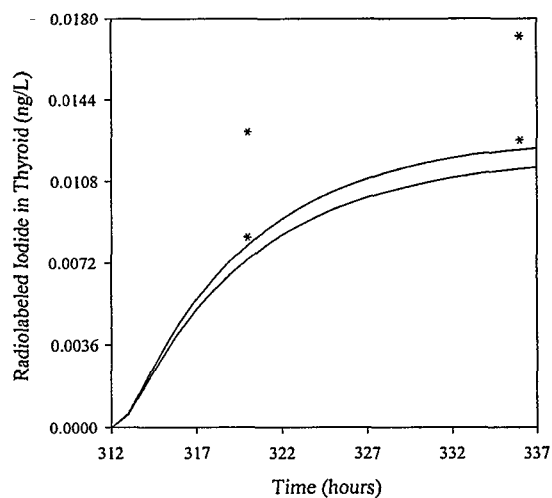
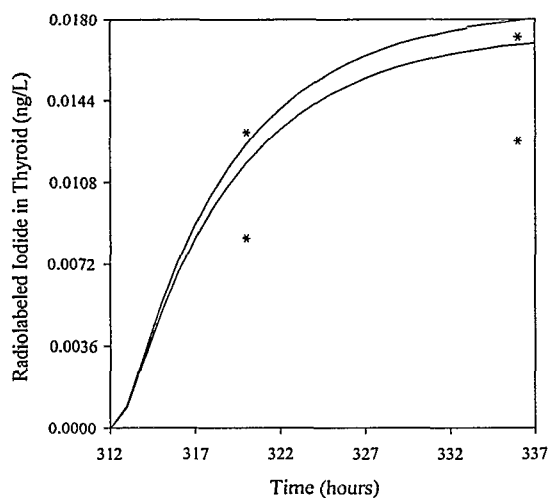


C. Thyroid radioiodide uptakes (before perchlorate) (top asterisks) and on day 14 of perchlorate exposure at 0.02 mg/kg-day (bottom asterisks) in a healthy male. Simulation on the left obtained by using individually fitted  $V_{maxc\_Ti}$  of  $8.0 \times 10^4$ . Right simulation obtained using average  $V_{maxc\_Ti}$ .

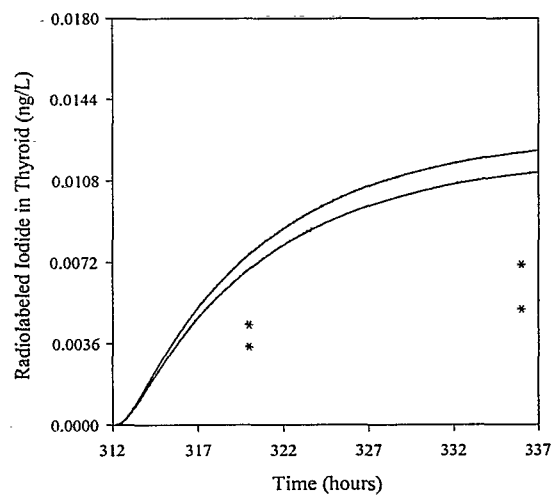
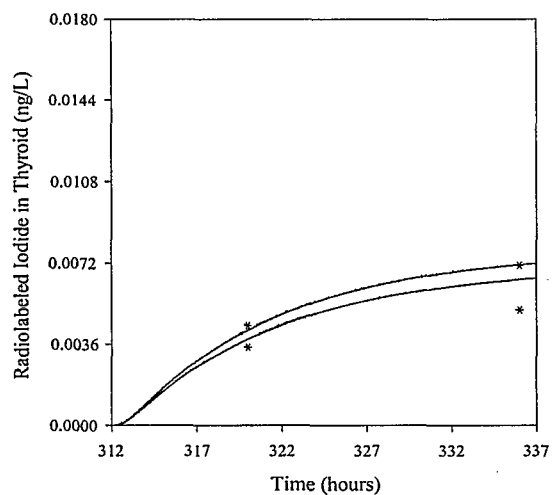


D. Thyroid radioiodide uptakes (before perchlorate) (top asterisks) and on day 14 of perchlorate exposure at 0.02 mg/kg-day (bottom asterisks) in a healthy female. Simulation on the left obtained by using individually fitted  $V_{maxc\_Ti}$  of  $1.5 \times 10^5$ . Right simulation obtained using average  $V_{maxc\_Ti}$ .

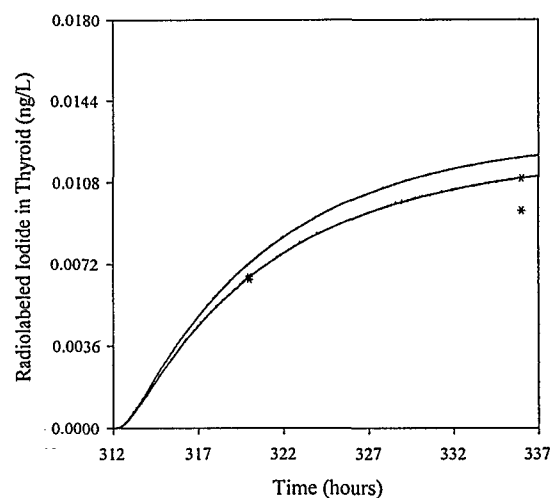
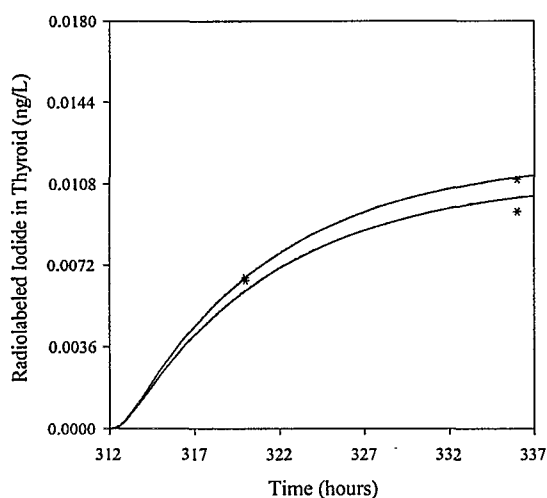
**Figure 13. Model predicted (lines) and observed 8 and 24 hour RAIU measurements (asterisks) during baseline (upper lines and asterisks) and on day 14 of perchlorate exposure at 0.02 mg/kg-day (lower lines and asterisks) from 4 healthy subjects. Individually fit thyroid uptakes for each subject are displayed in the plots on the left. Simulated thyroid uptakes using an average  $V_{maxc\_ti}$  of 150000 ng/hour-kg are displayed in the right plots (Greer *et al.*, 2000).**



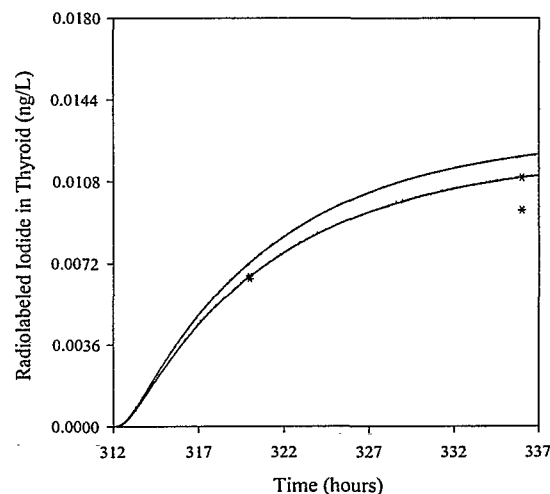
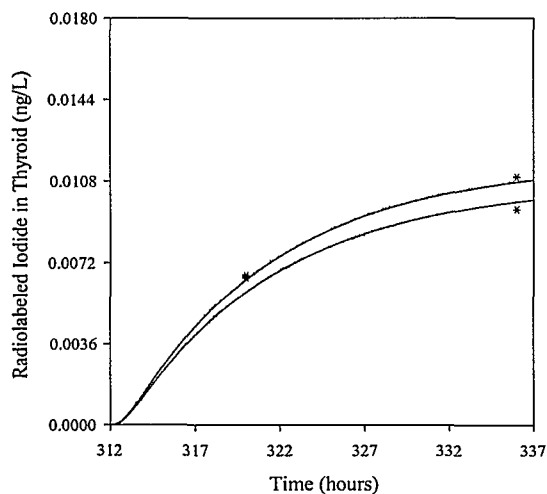
**A.** Thyroid radioiodide uptakes (before perchlorate) (top asterisks) and on day 14 of perchlorate exposure at 0.007 mg/kg-day (bottom asterisks) in a healthy female. Simulation on the left obtained by using individually fitted  $V_{maxc\_Ti}$  of  $2.8 \times 10^5$ . Right simulation obtained using average  $V_{maxc\_Ti}$ .



**B.** Thyroid radioiodide uptakes (before perchlorate) (top asterisks) and on day 14 of perchlorate exposure at 0.007 mg/kg-day (bottom asterisks) in a healthy female. Simulation on the left obtained by using individually fitted  $V_{maxc\_Ti}$  of  $7.8 \times 10^4$ . Right simulation obtained using average  $V_{maxc\_Ti}$ .



C. Thyroid radioiodide uptakes (before perchlorate) (top asterisks) and on day 14 of perchlorate exposure at 0.007 mg/kg-day (bottom asterisks) in a healthy male. Simulation on the left obtained by using individually fitted  $V_{maxc\_Ti}$  of  $1.35 \times 10^5$ . Right simulation obtained using average  $V_{maxc\_Ti}$ .



D. Thyroid radioiodide uptakes (before perchlorate) (top asterisks) and on day 14 of perchlorate exposure at 0.007 mg/kg-day (bottom asterisks) in a healthy female. Simulation on the left obtained by using individually fitted  $V_{maxc\_Ti}$  of  $1.35 \times 10^5$ . Right simulation obtained using average  $V_{maxc\_Ti}$ .

**Figure 14. Model predicted (lines) and observed 8 and 24 hour RAIU measurements (asterisks) during baseline (upper lines and asterisks) and on day 14 of perchlorate exposure at 0.007 mg/kg-day (lower lines and asterisks) from 4 healthy subjects. Individually fit thyroid uptakes for each subject are displayed in the left plots. Simulated thyroid uptakes using an average  $V_{maxc\_ti}$  of 150000 ng/hour-kg are displayed in the right plots (Greer *et al.*, 2000).**

The average  $V_{maxc\_Ti}$  fitted from Greer *et al.* (2000) ( $1.5 \times 10^5$  ng/hour-kg) agrees well with the value obtained from fitting data from Hays and Solomon (1965) ( $2.5 \times 10^5$  ng/hour-kg). The subjects in the Hays and Solomon study had fasted 12 hours prior to the administration of the *iv* radioiodide dose. As a result, intrathyroidal iodide levels would have been lower in the fasted individuals than in the individuals in the study by Greer *et al.* (2000), in which no dietary restrictions prior to thyroid uptake measurements were implemented. Therefore, the average  $V_{maxc\_Ti}$  from Hays and Solomon (1965) is expected to exceed that obtained from Greer *et al.* (2000).

Table 4 lists the average serum perchlorate concentrations and percent inhibitions from exposure day 14 from each dose group in the Greer *et al.* (2000) study described above. In addition, the average value for serum perchlorate concentration is provided from the unpublished study by Drs. Brabant and Leitoff, described previously in the Methods section. Simulations of data from this study are provided in the Model Validation section.

**Table 4. Average serum perchlorate and percent inhibition across dose groups in the 14-day drinking water studies**

Dose (mg/kg-day)	BW (kg)	Serum $ClO_4^-$ (mg/L)	Average % Inhibition of 24 hour Iodide Uptake <sup>4</sup>	Data Source
12.0	83.5 ± 17.4	23.0 ± 13.2	NA <sup>1</sup>	Unpublished data from Brabant and Leitolf, 2000
0.5	76.1 ± 14.3	0.649 ± 0.25	67.4 ± 12.1	Greer <i>et al.</i> , 2000
0.1	78.7 ± 13.2	0.126 ± .053	43.4 ± 12.3	Greer <i>et al.</i> , 2000
0.02	78.4 ± 18.2	<DL <sup>2</sup>	18.2 ± 12.8	Greer <i>et al.</i> , 2000
0.007	73.2 ± 15.4	NA <sup>3</sup>	6.0 ± 22.0	Greer <i>et al.</i> , 2000

NA = not available

<sup>1</sup>RAIU measurements were not taken in the unpublished 12 mg/kg/d study by Brabant and Leitolf.

<sup>2</sup> Samples at or below detection limit

<sup>3</sup>The 0.007 mg/kg/d dose was run to obtain inhibition data only. Serum and urine samples were not collected.

<sup>4</sup>Averages provided were calculated from exposure day 14 only.

## MODEL VALIDATION

The model was developed using the iodide kinetic data from Hays and Solomon (1965) and serum and urine perchlorate data with radioiodide uptake and inhibition measurements in the thyroid provided by Greer and associates (2000). The ability of the model to predict human data



from other experiments, analyzed at different labs, was tested using available data from independent studies.

Using the parameters in Table 2, the model adequately simulated cumulative perchlorate in urine reported in three published studies using therapeutic perchlorate dose levels (Figures 15 through 17). Oral doses administered in these studies were approximately 9.07 mg/kg (Durand, 1938), 9.56 mg/kg (Kamm and Drescher, 1973) and 20 mg/kg (Eichler, 1929). The previously determined urinary clearance value (ClUc<sub>p</sub>) of 0.126 L/hour-kg was used with all validation data.

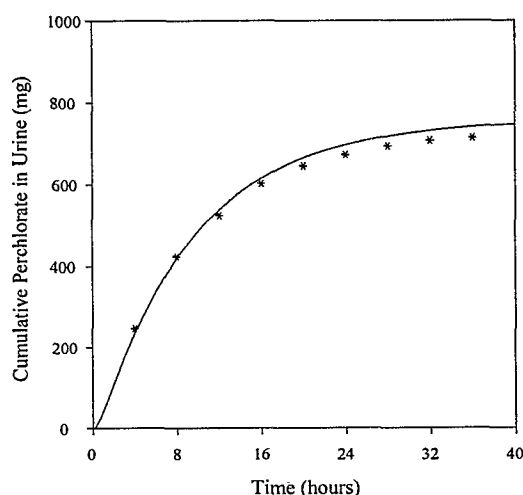


**Figure 15. Model predicted (line) and observed (circles) cumulative  $\text{ClO}_4^-$  in urine from a healthy male after an oral dose of 9.56 mg  $\text{ClO}_4^-$  (Kamm and Drescher, 1973). Simulation obtained by using parameters in Tables 1 and 2.**

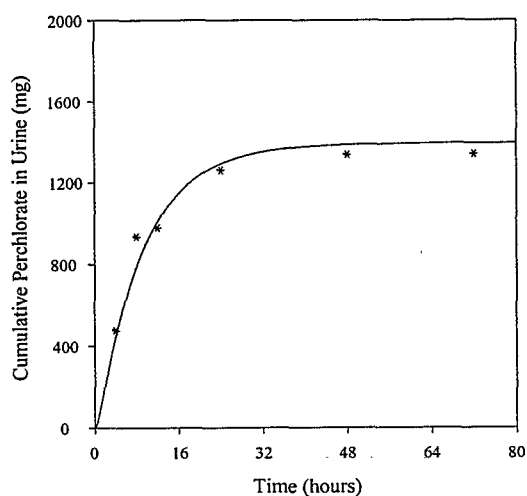


**Figure 16. Model predicted (line) and observed (circles) cumulative  $\text{ClO}_4^-$  in urine from a healthy male after an oral dose of approximately 20 mg  $\text{ClO}_4^-$  /kg (Eichler, 1929). Simulation was obtained by using the parameters in Tables 1 and 2.**

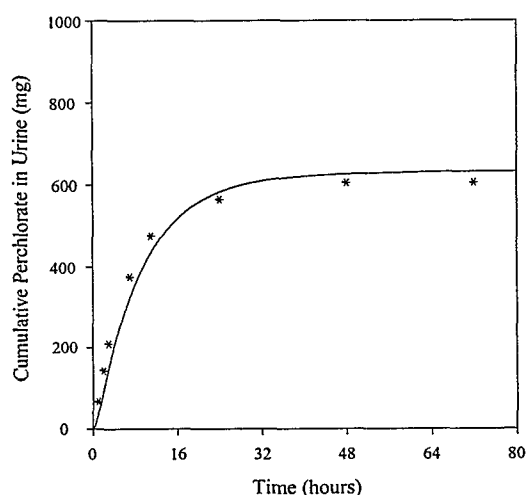
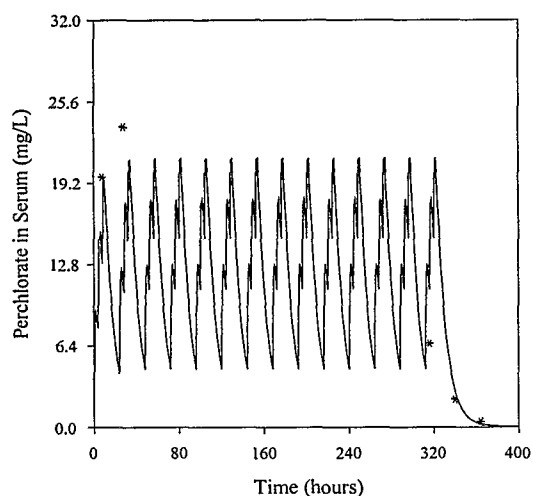


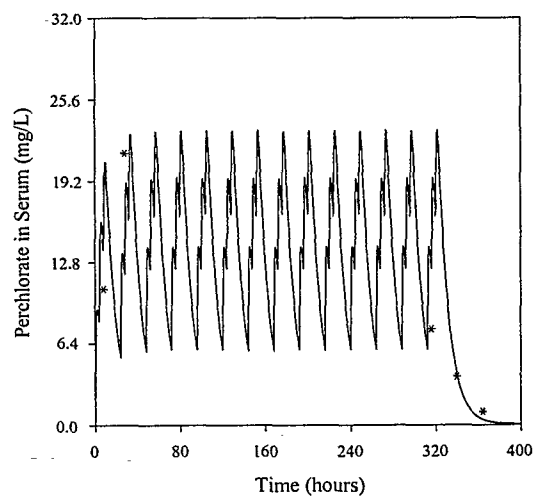
**Figure 17. Model predicted (line) and observed (circles) cumulative amount of  $\text{ClO}_4^-$  in urine from a healthy male after an oral dose of approximately 9.07 mg/kg  $\text{ClO}_4^-$  (Durand, 1938). Simulation obtained by using the parameters in Tables 1 and 2.**

The ability of the model to predict cumulative perchlorate in urine from three different studies at three different doses with the same set of parameters, established from the studies by Hays and Solomon (1965) and Greer *et al.* (2000), demonstrates the usefulness of the model. In addition it provides validation for the model structure and physiological and chemical parameters used.

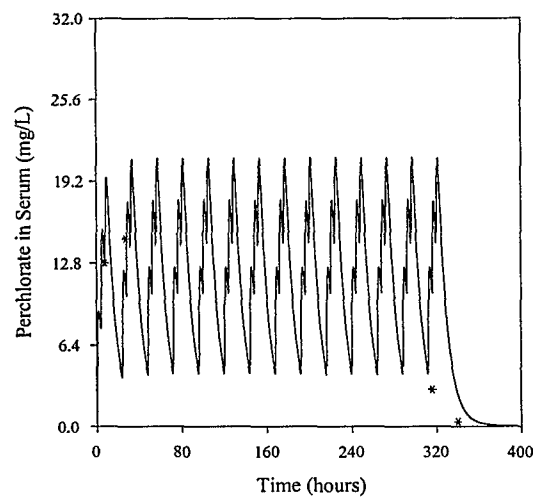
The model also predicts serum perchlorate concentrations at 12 mg/kg-day from an unpublished study performed by Dr. Georg Brabant at the Medizinische Hochschule, Hanover, Germany (Figure 18). This study was very similar to Greer *et al.* (2000). Subjects received 12 mg/kg-day perchlorate in drinking water near meal times. Variability in the observed serum measurements is believed to reflect variability in the dosing regime, as the experimental protocol was less fixed than that used in Greer *et al.* (2000). Again the usefulness of the model is demonstrated by its ability to successfully predict serum concentrations from a dose 24 times higher than the high dose used to establish perchlorate parameters (0.5 mg/kg-day).



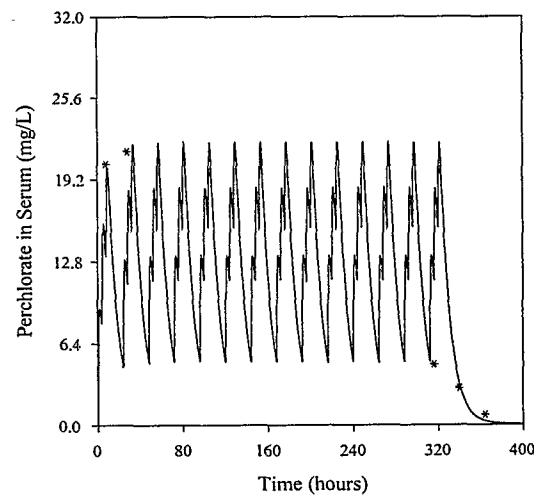
A



B



C



D

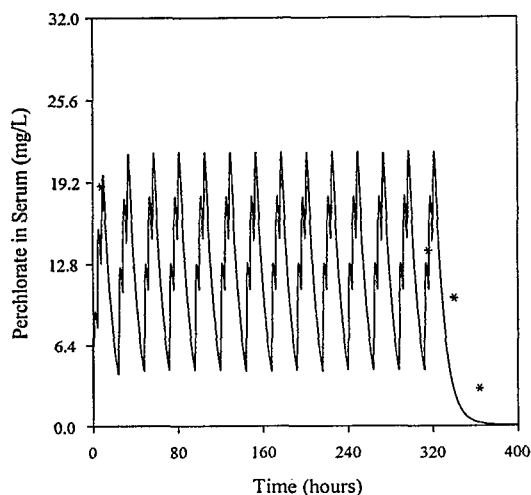


**Figure 18. Serum perchlorate concentrations in 5 males during exposure to 12 mg/kg-day  $\text{ClO}_4^-$  in drinking water. Subjects were instructed to ingest the drinking water solution 3 times/day for 14 days. Serum samples were collected at approximately 2 hours after the first dose, after 12 pm on day two, the morning of day 14 and post exposure days 1 and 2 (unpublished data, Brabant and Leitolf).**

**E**

The model successfully simulates the thyroidal iodide uptake in a subject with hyperthyroidism by increasing the maximum velocity in the follicular epithelium ( $V_{\text{maxc\_Ti}}$ ) to  $5.0\text{E}6$  ng/L-kg, a factor of ten times higher than in normal subjects (upper line in Figure 19). This increase in  $V_{\text{maxc\_Ti}}$  is supported in the literature, as Gluzman and Niepomnischce (1983) measured elevated  $V_{\text{max}}(s)$  in thyroid specimens from subjects with Grave's disease. That the model is capable of predicting uptake under this condition supports the usefulness of the current model structure.

The model underpredicts the degree of inhibition caused by perchlorate in this subject (bottom line Figure 19). It would appear that the increased inhibition could be attributed to a lower  $K_m$  value. However, Gluzman and Niepomnischce (1983) noted that the  $K_m$  did not differ greatly between thyroid specimens from hyperthyroid subjects and normal subject. This suggests that the increased inhibition by perchlorate seen in Grave's disease may be attributed to a mechanism other than NIS affinity.

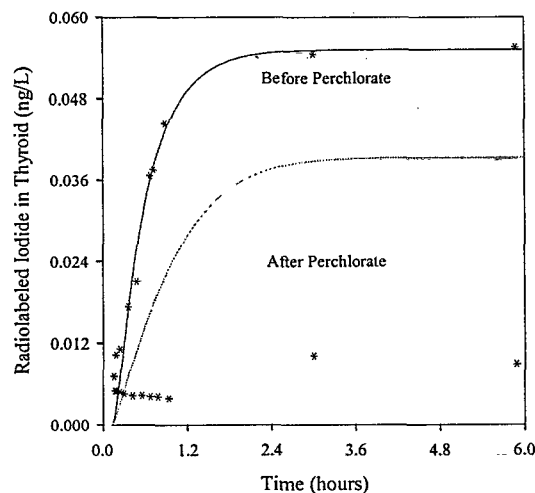


**Figure 19. Model predicted (line) and observed (asterisks) amount of  $^{131}\text{I}^-$  uptake in the thyroid of a male with Graves after *iv* dose of  $10\ \mu\text{Ci}\ ^{131}\text{I}^-$  before and after  $100\ \text{mg}\ \text{KClO}_4^-$  (Stanbury and Wyngaarden, 1952).**

## SUMMARY AND CONCLUSIONS

The model adequately simulates serum concentrations and cumulative urine after drinking water exposure to perchlorate spanning four orders of magnitude ( $0.02$  to  $12.0\ \text{mg/kg-day}$ ). Serum perchlorate levels were not available at  $0.02\ \text{mg/kg-day}$ ; however the model did predict the cumulative urine from that dose group (Figure 10). The model slightly underpredicts serum levels at  $0.1\ \text{mg/kg-day}$  (Figure 9). It is possible that binding with some serum proteins occurs to a greater extent than demonstrated in this model; however, increasing binding does not allow fitting of the urine data at that dose level, so it's possible that less uptake in one or more tissues is actually occurring.

Aspects of the model, which were supported in the literature or laboratory studies but which could not be directly observed in humans, were incorporated if necessary to improve fits. For example, the slow diffusion of iodide and active uptake of perchlorate into human skin was incorporated in spite of a lack of available human data to support them. However, the model required the inclusion of active uptake in human skin. Without the skin compartment, the model overestimated circulating plasma inorganic iodide and perchlorate. As discussed earlier, cutaneous uptake of iodide and perchlorate in mice and rats has been reported (Brown-Grant and Pethes, 1959; Zeghal *et al.*, 1995). The lack of reported iodide in human skin from clinical radioiodide scans may be due to difficulty in differentiating it from background radioactivity. However, due to its large size, skin appears to be an important pool for slow turnover of iodide.

Early iodide kinetics were established by fitting data from Hays and Solomon (1965), as described previously. Interestingly, the simulated amount of  $^{131}\text{I}^-$  in gastric juice (simulated control session) indicates rapid uptake of iodide (and likely perchlorate as well) into this

compartment and quick reabsorption in the tissue (Figure 2C). GI clearance of iodide is rapid and plays an important role in radioiodide conservation.

The appearance of time-course radioiodine in stomach contents of any species is complicated by the fact that it reflects more than sequestration of radioiodide by NIS. Its appearance also reflects radioiodide contributed through the gradual accumulation of iodide in saliva that is swallowed involuntarily throughout the study. Several studies that examined sequestration of these anions in digestive juices have all shown high variability in the concentrations measured over time (Honour *et al.*, 1952; Hays and Solomon, 1965; Merrill, 2001). There is a tendency for the gastric juice to plasma ratio to be low when the rate of secretion of juice is high (Honour *et al.*, 1952). Fluctuations in the secretion rate are probably the most important factor in determining the pattern of the concentration ratios in individuals. Therefore, variability in stomach or GI tract parameters between models is expected. However, the early rise in the gastric juice:plasma ratio mentioned earlier is a constant feature across these data sets, whether or not an attempt was made to eliminate contamination of gastric juices by dietary contents or saliva. The model successfully predicts this same trend.

Variability across data sets was noted in the mean  $V_{maxc\_Ti}$  values, ranging from  $5.0E4$  to  $5.0E5$  ng/hour-kg. These values were estimated from best visual fits of baseline 8 and 24 hour thyroid RAIU data. Inhibition data from higher dose groups would be useful to test the robustness of the model to predict inhibition of uptake of iodide in the thyroid.

Average urinary clearance values were found to be 0.1 L/hour-kg for iodide and 0.126 L/hour-kg for perchlorate. Excretion constants were highest among the 0.1 mg/kg-day group. With the urinary excretion rates fitted to cumulative urine data, the model tends to slightly underestimate serum perchlorate levels at repeated low doses. Elevated serum concentrations may indicate plasma binding of perchlorate. Yamada and Jones (1967) studied effects of different anions on plasma binding to thyroxine and noted that some of the thyroxine had been displaced after perchlorate was introduced. Thus, it is possible that perchlorate competes with thyroxine for the same binding sites of plasma proteins (Merrill, 2001; Clewell, 2001a).

Dietary iodine and endogenous inorganic iodide levels are clearly important in modeling iodide and perchlorate kinetics, because excessive iodide levels cause the ion to inhibit its own uptake. Plasma inorganic iodide (PII) is rarely reported in the literature, due to analytical difficulties, and it was not available in any of the studies presented in this paper. While measurements of tracer radioiodide can be fitted to predict transfer rates, its use is limited when attempting to predict the saturation of nonlinear compartments, such as the thyroid, which are dependent upon the existing amount of iodide already present. Subsequent modeling efforts on predicting subsequent effects of iodide inhibition on thyroid hormone synthesis and regulation in humans will require the capability of the model to predict PII. Ultimately, regional dietary iodine should be considered in creating recommendations on drinking water levels for perchlorate.

Statistical analyses were performed on the hormone data collected from Greer *et al.* (2000). Details on the statistical analyses are provided in Attachment 2. In summary, there was little effect of perchlorate on levels of  $T_4$ , free  $T_4$  or  $T_3$ . TSH decreased significantly from baseline by

exposure day 3. On post exposure day 1, the TSH levels of the subjects in the 0.5 mg/kg-day group had decreased by an average of 35% from baseline (ranging from 17% to 52%). Therefore, it appears that TSH was dropping while inhibition remained the same. It is possible that there is an increase in thyroid sensitivity to TSH as an early response to inhibition (Brabant *et al.*, 1992). This increased sensitivity (possibly an increase affinity of the TSH receptor) could possibly decrease circulating TSH levels, while  $T_4$  has not decreased sufficiently yet to stimulate the hypothalamus to increased TRH secretions. After perchlorate was discontinued, between post exposure days 1 and 15, the mean TSH level increased significantly over baseline (23% greater than baseline), with TSH of one subject remaining below baseline. The drop in TSH during perchlorate exposure and the rise above baseline measurements after perchlorate are the opposite of the TSH regulation expected and are unexplained at this point.

In addition, the data by Greer *et al.* (2000) showed an increase in radioiodide uptake in excess of baseline measurements 14 days after perchlorate exposure. An increase in radioiodide uptake is expected due to the rise in TSH mentioned above. This rebound effect has been noted in other human inhibition studies (using both iodide and perchlorate as inhibitors). Saxena *et al.* (1962) evaluated the prophylactic doses of iodide required to suppress thyroid uptake of  $^{131}\text{I}$  in euthyroid mentally defective children. They found a minimal effective oral dose of 1500 to 2000  $\mu\text{g}$  iodide per square meter of body surface per day was required to completely suppress  $^{131}\text{I}$  uptake. Within a week after iodide administration was stopped, a rebound of uptake was noted. In some instances these uptakes were even higher in subsequent weeks.

The PBPK models developed for perchlorate induced inhibition may ultimately be used to evaluate the dose-response of adverse effects from low level perchlorate exposure. Modeled effects on hormone regulation are yet to be developed. Perturbations in hormones levels after perchlorate exposure demonstrate complex differences in the hormone regulatory mechanisms between rats and humans, which are difficult to describe (Merrill, 2001; Clewell, 2001a and 2001b). However, the current model structures may also provide a basis for evaluating thyroid effects from other environmental contaminants. For example, excessive exposure to other similarly behaving anions, such as nitrate (a frequently found contaminant in drinking water supplies), may contribute to antithyroid effects (Wolff and Maurey, 1963).

## ACKNOWLEDGEMENTS

The authors express special thanks to Drs. Monte Greer, Gay Goodman, Georg Brabant and Holger Leitolf for providing serum and urine samples from their experiments and sharing their results. Also acknowledged are Lt Col Dan Rogers, Dr. Richard Stotts and Dr. Dave Mattie, U.S. Air Force, for assistance in obtaining funding of this research and Mel Andersen (Colorado State University, Fort Collins, CO), Harvey Clewell (ICF Consulting, Ruston, LA) and Annie Jarabek (NCEA, USEPA, RTP, NC) for expert advice. The authors would also like to acknowledge Charles Goodyear for performing statistical analyses of the data. Mr. Goodyear is a statistical consultant for AFRL, Human Effectiveness Directorate, Crew Systems Interface Division (AFRL/HEC), Wright-Patterson AFB, OH. Lastly, in-house work would not have been possible without analytical support from Lt Eric Eldridge (AFRL/HEST, WPAFB, OH), Latha Narayanan

(GEOCENTERS, Inc, WPAFB, OH), Gerry Buttler (ManTech Environmental Technology, Dayton, OH) and SSgt Paula Todd (AFRL/HEST, WPAFB, OH).

## REFERENCES

Ajjan, R.A., Kamaruddin, N.A., Crisp, M., Watson, P.F., Ludgate, M., and Weetman, A.P., 1998, Regulation and tissue distribution of the human sodium iodide symporter gene: Clin.Endocrinol., 49, p. 517-523.

Altman, P.L. and Dittmer, D.S., 1971a, Blood volumes: (147):p. 376-383. Respiration and Circulation. Federation of American Societies for Experimental Biology: Bethesda, MD.

Altman, P.L. and Dittmer, D.S., 1971b, Volume of blood in tissue: Vertebrates:(148):p. 383-387. Respiration and Circulation. Federation of American Societies for Experimental Biology: Bethesda, MD.

Anbar, M., Guttmann, S., and Lewitus, Z., 1959, The mode of action of perchlorate ions on the iodine uptake of the thyroid gland: Int.J.Appl.Radiat.Isot., 7, p. 87-96.

Bagchi, N. and Fawcett, D.M., 1973, Role of sodium ion in active transport of iodide by cultured thyroid cells: Biochim.Biophys.Acta, 318, p. 235-251.

Brabant, G., Bergmann, P., Kirsch, C.M., Kohrle, J., Hesch, R.D., and von zur Muhlen, A., 1992, Early adaptation of thyrotropin and thyroglobulin secretion to experimentally decreased iodine supply in man: Metabolism, 41, p. 1093-1096.

Brown, R.A., Al-Moussa, M., and Beck, J., 1986, Histometry of normal thyroid in man: J.Clin.Pathol., 39, p. 475-482.

Brown, R.P., Delp, M.D., Lindstedt, S.L., Rhomberg, L.R., and Beliles, R.P., 1997, Physiological parameter values for physiologically based pharmacokinetic models: Toxicol.Ind.Health, 13, p. 407-484.

Brown-Grant, K., 1961, Extrathyroidal iodide concentrating mechanisms: Physiolog.Rev., 41, p. 189-213.

Brown-Grant, K. and Pethes, G., 1959, Concentration of radio-iodide in the skin of the rat: J.Physiol., 148, p. 683-693.

Carrasco, N., 1993, Iodide transport in the thyroid gland: Biochim.Biophys.Acta, 1154, p. 65-82.



Cavalieri, R.R., 1997, Iodine metabolism and thyroid physiology: current concepts: *Thyroid*, 7, p. 177-181. Chow, S.Y. and Woodbury, D.M., 1970, Kinetics of distribution of radioactive perchlorate in rat and guinea-pig thyroid glands: *J.Endocrinol.*, 47, p. 207-218.

Chow, S.Y., Chang, L.R., and Yen, M.S., 1969, A comparison between the uptakes of radioactive perchlorate and iodide by rat and guinea-pig thyroid glands: *J.Endocrinol.*, 45, p. 1-8.

Clewell, R.A., 2001a, Physiologically-based pharmacokinetic model for the kinetics of perchlorate-induced inhibition of iodide in the pregnant rat and fetus: Human Effectiveness Directorate, Operational Toxicology Branch, Wright-Patterson AFB, OH. AFRL-HE-WP-CL-2001-0006.

Clewell, R.A., 2001b, Physiologically-based pharmacokinetic model for the kinetics of perchlorate-induced inhibition of iodide in the lactating and neonatal rat: Human Effectiveness Directorate, Operational Toxicology Branch, Wright-Patterson AFB, OH. AFRL-HE-WP-CL-2001-0007.

Crump, C., Michaud, P., Tellez, R., Reyes, C., Gonzalez, G., Montgomery, E.L., Crump, K.S., Lobo, G., Becerra, C., and Gibbs, J.P., 2000, Does perchlorate in drinking water affect thyroid function in newborns or school-age children?: *J.Occup.Environ.Med.*, 42, p. 603-612.

Durand, J., 1938, Recherches sur l'elimination des perchlorates, sur leur repartition dans les organes et sur leur toxicite [Research on the elimination of perchlorate, its distribution in organs and its toxicity]: *Bull.Soc.Chim.Biol.*, 20, p. 423-433.

Eichler, O., 1929, Zur Pharmakologie der Perchloratwirkung [The pharmacology of the perchlorate effect]: *Naunyn-Schmiedeberg's Arch.Exp.Path.u.Pharmak*, 144, p. 251-260.

Fisher, J., Todd, P., Mattie, D., Godfrey, D., Narayanan, L., and Yu, K., 2000, Preliminary development of a physiological model for perchlorate in the adult male rat: a framework for further studies: *Drug Chem.Toxicol.*, 23, p. 243-258.

Gibbs, J.P., Ahmad, R., Crump, K.S., Houck, D.P., Leveille, T.S., Findley, J.E., and Francis, M., 1998, Evaluation of a population with occupational exposure to airborne ammonium perchlorate for possible acute or chronic effects on thyroid function: *J.Occup.Environ.Med.*, 40, p. 1072.

Gluzman, B.E. and Niepomnische, H., 1983, Kinetics of the iodide trapping mechanism in normal and pathological human thyroid slices: *Acta Endocrinol.*, 103, p. 34-39.

Golstein, P., Abramow, M., Dumont, J.E., and Beauwens, R., 1992, The iodide channel of the thyroid: a plasma membrane vesicle study: *Am.J.Physiol.*, 263, p. C590-7.

Granger, D.N., Barrowman, J.A., and Kviety, P.A., 1985, *Clinical Gastrointestinal Physiology*: W.B. Saunders Company, Philadelphia.

Greer, M.A., Goodman, G., Pleus, R.C., and Greer, S.E., 2000, Does environmental perchlorate exposure alter human thyroid function? Determination of the dose-response for inhibition of radioiodine uptake: *Endocrine.J.*, 40(Suppl 1, p. 148. (Abstract)

Halmi, N.S. and Stuelke, R.G., 1959, Comparison of Thyroidal and Gastric Iodide Pumps in Rats: *Endocrinology*, 64, p. 103-109.

Halmi, N.S., Stuelke, R.G., and Schnell, M.D., 1956, Radioiodide in the thyroid and in other organs of rats treated with large doses of perchlorate: *Endocrinology*, 58, p. 634-650.

Hanwell, A. and Linzell, J.L., 1973, The time course of cardiovascular changes in lactation in the rat: *J Physiol.Lond.*, 233, p. 93-109.

Harden, R.G., Alexander, W.D., Shimmins, J., and Robertson, J.W., 1968, A comparison between the inhibitory effect of perchlorate on iodide and pertechnetate concentrations in saliva in man: *Q.J.Exp.Physiol.Cogn.Med.Sci.*, 53, p. 227-238.

Hays, M.T. and Green, F.A., 1973, In vitro studies of <sup>99m</sup>Tc-pertechnetate binding by human serum and tissues: *J.Nucl.Med.*, 14, p. 149-158.

Hays, M.T. and Solomon, D.H., 1965, Influence of the gastrointestinal iodide cycle on the early distribution of radioactive iodide in man: *J.Clin.Invest.*, 44, p. 117-127.

Hays, M.T. and Wegner, L.H., 1965, A mathematical and physical model for early distribution of radioiodide in man: *J.Appl.Physiol.*, 20, p. 1319-1328.

Honour, A.J., Myant, N.B., and Rowlands, E.N., 1952, Secretion of radioiodine in digestive juices and milk in man: *Clin.Sci.*, 11, p. 447-463.

Kamm, G. and Drescher, G., 1973, [Demonstration of perchlorate in the urine.] Der Nachweis von Perchlorat im Urin: *Beitr.Gerichtl.Med.*, 30, p. 206-210.

Kotani, T., Ogata, Y., Yamamoto, I., Aratake, Y., Kawano, J.I., Suganuma, T., and Ohtaki, S., 1998, Characterization of gastric Na<sup>+</sup>/I<sup>-</sup> symporter of the rat: *Clin.Immunol.Immunopathol.*, 89, p. 271-278.

Lamm, S.H. and Doemland, M., 1999, Has perchlorate in drinking water increased the rate of congenital hypothyroidism: *J.Occup.Environ.Med.*, 41, p. 409-411.

Laurberg, P., Nohr, S.B., Pedersen, K.M., Hreidarsson, A.B., Andersen, S., Bulow, P., I, Knudsen, N., Perrild, H., Jorgensen, T., and Ovesen, L., 2000, Thyroid disorders in mild iodine deficiency: *Thyroid* 2000, 10, p. 951-963.

Lazarus, J.H., Harden, R.M., and Robertson, J.W., 1974, Quantitative studies of the inhibitory effect of perchlorate on the concentration of  $^{36}\text{ClO}$  minus  $^{125}\text{I}$  minus and  $^{99\text{m}}\text{TcO}$  minus 4 in salivary glands of male and female mice: *Arch.Oral Biol.*, 19, p. 493-498.

Leggett, R.W. and Williams, L.R., 1995, A proposed blood circulation model for Reference Man: *Health Phys.*, 69, p. 187-201.

Li, Z., Li, F.X., Byrd, D., Deyhle, G.M., Sesser, D.E., Skeels, M.R., and Lamm, S.H., 2000, Neonatal thyroxine level and perchlorate in drinking water: *J.Occup.Environ.Med.*, 42, p. 200-205.

Licht, W.R. and Deen, W.M., 1988, Theoretical model for predicting rates of nitrosamine and nitrosamide formation in the human stomach: *Carcinogenesis*, 9, p. 2227-2237.

Malik, A.B., Kaplan, J.E., and Saba, T.M., 1976, Reference sample method for cardiac output and regional blood flow determinations in the rat: *J Appl.Physiol.*, 40, p. 472-475.

Marieb, E., 1992, *Human Anatomy and Physiology*. Second Edition: Benjamin/Cummings Publishing Company, Inc., Redwood City, California.

Merrill, E.A., 2000, Human PBPK Model for Perchlorate Inhibition of Iodide Uptake in the Thyroid: Human Effectiveness Directorate, Operational Toxicology Branch, Wright-Patterson AFB, OH. AFRL-HE-WP-CL-2000-0036.

Merrill, E.A., 2001, PBPK Model for Perchlorate-Induced Inhibition in the Male Rat: Human Effectiveness Directorate, Operational Toxicology Branch, Wright-Patterson AFB, OH. AFRL-HE-WP-CL-2001-0005.

Pena, H.G., Kessler, W.V., Christian, J.E., Cline, T.R., and Plumlee, M.P., 1976, A comparative study of iodine and potassium perchlorate metabolism in the laying hen. 2. Uptake, distribution, and excretion of potassium perchlorate: *Poult.Sci.*, 55, p. 188-201.

Perlman, I., Chaikoff, I.L., and Morton, M.E., 1941, Radioactive iodine as an indicator of the metabolism of iodine. I. The turnover of iodine in the tissues of the normal animal, with particular reference to the thyroid: *J.Biol.Chem.*, 139, p. 433-447.

Porterfield, S.P., 1994, Vulnerability of the developing brain to thyroid abnormalities: environmental insults to the thyroid system: *Environ.Health Perspect.*, 102 Suppl 2, p. 125-130.

Rall, J.E., Power, M.H., and Albert, A., 1950, Distribution of radioiodine in erythrocytes and plasma of man: *Proc.Soc.Exp.Biol.Med.*, 74, p. 460-461.

Saxena, K.M., Chapman, E.M., and Pryles, C.V., 1962, Minimal dosage of iodide required to suppress uptake of iodine-131 by normal thyroid: *Science*, 138, p. 430-431.

- Scatchard, G. and Black, E.S., 1949, The effect of salts on the isoionic and isoelectric points of proteins: *J.Phys.Colloid Chem.*, 53, p. 88-99.
- Spitzweg, C., Heufelder, A.E., and Morris, J.C., 2000, Thyroid iodine transport: *Thyroid*, 10, p. 321-330.
- Spitzweg, C., Joba, W., Eisenmenger, W., and Heufelder, A.E., 1998, Analysis of human sodium iodide symporter gene expression in extrathyroidal tissues and cloning of its complementary deoxyribonucleic acids from salivary gland, mammary gland, and gastric mucosa: *J.Clin.Endocrinol.Metab.*, 83, p. 1746-1751.
- Stanbury, J.B. and Wyngaarden, J.B., 1952, Effect of perchlorate on the human thyroid gland: *Metabolism*, 1, p. 533-539.
- Urbansky, E.T. and Schock, M.R., 1999, Issues in managing the risks associated with perchlorate in drinking water: *J.Environ.Management*, 56, p. 79-95.
- Wolff, J., 1998, Perchlorate and the Thyroid Gland: *Pharmacolog.Rev.*, 50, p. 89-105.
- Wolff, J. and Maurey, J.R., 1961, Thyroidal iodide transport: II. Comparison with non-thyroid iodide-concentrating tissues: *Biochim.Biophys.Acta*, 47, p. 467-474.
- Wolff, J. and Maurey, J.R., 1963, Thyroidal Iodide Transport: IV. The Role of Ion Size: *Biochim.Biophys.Acta*, 69, p. 48-58.
- Wyngaarden, J.B., Wright, B.M., and Ways, P., 1952, The effect of certain anions upon the accumulation and retention of iodide by the thyroid gland: *Endocrinology*, 50, p. 537-549.
- Yamada, T. and Jones, A.E., 1968, Effect of thiocyanate, perchlorate and other anions on plasma protein-thyroid hormone interaction in vitro: *Endocrinology*, 82, p. 47-53.
- Yokoyama, N., Nagayama, Y., Kakezono, F., Kiriya, T., Morita, S., Ohtakara, S., Okamoto, S., Morimoto, I., Izumi, M., Ishikawa, N., and et al., 1986, Determination of the volume of the thyroid gland by a high resolutional ultrasonic scanner: *J.Nucl.Med.*, 27, p. 1475-1479.
- Yu, K.O., 2000, Tissue distribution and inhibition of iodide uptake in the thyroid by perchlorate with corresponding hormonal changes in pregnant and lactating rats (drinking water study): Human Effectiveness Directorate, Operational Toxicology Branch, Wright-Patterson AFB, OH. AFRL-HE-WP-CL-2000-0038.
- Yu, K.O., Todd, P.N., Bausman, T.A., Young, S.M., Mattie, D.R., Fisher, J.W., Narayanan, L., Godfrey, R.J., Goodyear, C.D. and Sterner, T.R., 2000, Effects of perchlorate on thyroidal uptake of iodide with corresponding hormonal changes: Human Effectiveness Directorate, Operational Toxicology Branch, Wright-Patterson AFB, OH. AFRL-HE-WP-TR-2000-0076.

Zeghal, N., Redjem, M., Gondran, F., and Vigouroux, E., 1995, [Analysis of iodine compounds in young rat skin in the period of suckling and in the adult. Effect of perchlorate]. Analyse des composés iodés de la peau chez le jeune rat en période d'allaitement et chez l'adulte. Effet du perchlorate: Arch.Physiol.Biochem., 103, p. 502-511.

## ATTACHMENT 2

### Serum Hormones (TSH, T<sub>3</sub>, T<sub>4</sub>, fT<sub>4</sub>) Statistical Analysis

Charles D. Goodyear

Twenty-four subjects (12 male and 12 female) participated in the 2000 study by Greer and colleagues. Each subject had their hormone levels (TSH, T<sub>4</sub>, free T<sub>4</sub> and T<sub>3</sub>) determined on a screening day and a baseline day. At this time, the subjects were randomly assigned to one of 3 dose groups (0.02, 0.1 and 0.5 mg/kg-day) such that there were 4 male and 4 female subjects in each group. An additional dose group (0.007 mg/kg-day) was included for inhibition measurement but no serum samples were collected besides preliminary screening samples. Over the next 2 weeks, each subject was dosed with perchlorate, using drinking water, at different times on days 1, 2, 3, 4, 8 and 14. Before drinking perchlorate, blood was drawn to determine their hormone levels. Lastly, blood was drawn 1 and 15 days post exposure. For all subjects, exposure day 1 was 5 days after baseline.

Table 1. Times of blood draws

Exposure Day	Time Period	# Subjects
Baseline	1	24
1	2	23
	3	24
2	1	23
	2	23
	3	24
3	1	24
4	1	23
	2	24
8	1	15
	2	7
	3	2
14	1	24
	2	24
	3	24
Post 1	1	24
Post 15	1	24

Time periods were: 1 = 0800 - 0955 hours, 2 = 1010 - 1405 hours and 3 = 1450 - 1946 hours. The only exception was one Post 1 blood draw at 1024 (listed as time period = 1). The time 1946 hours is most likely the recording time instead of the draw time.

On exposure day 8, each subject had blood drawn only once, at different times throughout the day. The purpose of the analyses was to determine: 1) Do the dose groups differ, at each exposure day separately, in their percent change from baseline? 2) Do the males and females differ, at each exposure day separately, in their percent change from baseline? 3) What combinations of dose group and exposure day show a significant change from baseline. Baseline means and standard deviations of subjects are shown in Table 2.

**Table 2. Baseline mean and standard deviation of subjects (N=24)**

<b>Hormone</b>	<b>Mean</b>	<b>SD</b>
TSH ( $\mu$ U/mL)	2.16	1.01
T <sub>4</sub> ( $\mu$ g/dL)	7.34	1.75
free T <sub>4</sub> (ng/dL)	1.16	0.17
T <sub>3</sub> (ng/dL)	105.25	15.70

Since blood was drawn at different times during the exposure days, time of day needs to be addressed as a factor, especially since previous research has shown time of day to be an influence (Brabant *et al.*, 1992a and 1992b). A preliminary screening occurred 1 to 34 days before baseline with most subjects screened less than 10 days before baseline. Figure 1 contains the screening day hormone level percent change from the baseline hormone level. All baseline blood draws were between 0800 and 0908. The X-axis values represent the time of day for the screening blood draw. For T<sub>4</sub>, free T<sub>4</sub> and T<sub>3</sub>, time of day does not appear to be related to hormone level for comparing the screening day and the baseline day. For TSH, most subjects who had blood drawn after 1000 on the screening day showed lower hormone levels compared with the baseline day.

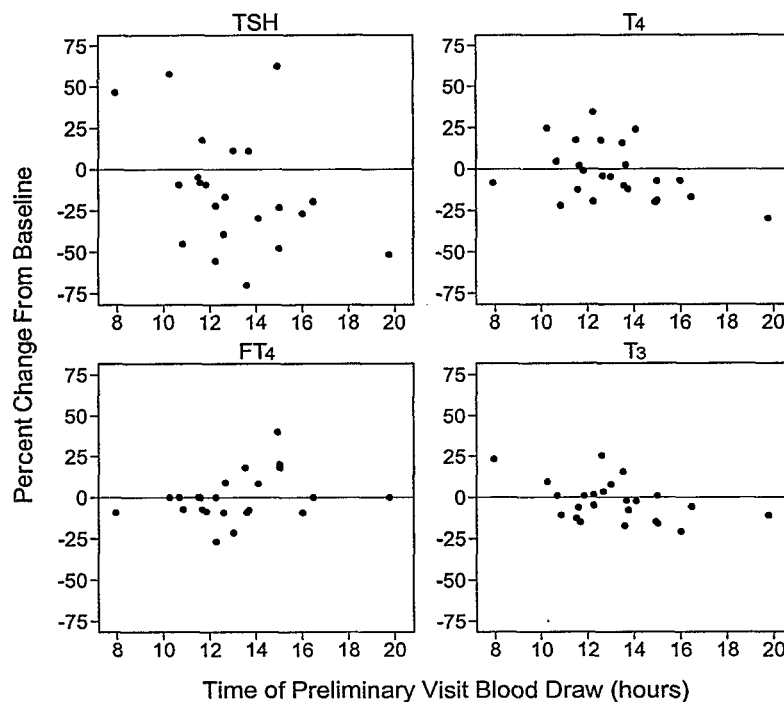


**Figure 1. Percent change from baseline to the preliminary visit for the 24 subjects. The time of 1946 is most likely recording time instead of draw time.**

Analyses of variance were performed on exposure days 1, 2, 4 and 14, for each dose group separately, to help indicate whether time of day might be related to a change in hormone level. The dependent variable was percent change from baseline. These tests indicated that time of day may influence hormone levels, particularly for TSH. As with the comparisons of screening and baseline days, the TSH level appears to decrease from the morning to the afternoon. This circadian trend in TSH has been documented (Brabant *et al.*, 1992a and 1992b). All further analyses, tables and figures used data from the morning blood draws only (i.e., time period = 1) as the baseline blood draws were in the morning. A thorough analysis of the effects of time of day will not be performed here.

To compare the dose groups and sexes, at each exposure day separately, a two-factor analysis of variance was performed. The dependent variable was the percent change from baseline. Post-hoc paired comparisons of the dose groups used the Bonferroni procedure with a family-wise error level of 0.05. Tables 3 through 6 show results of these analyses. The error degrees of freedom indicate missing data (i.e., DFE = 18 indicates no missing data). For exposure day 8, there was only 15 subjects, 3 female and 2 male in the 0.02 and 0.1 mg/kg-day dose groups, 2 female and 3 male in the 0.5 mg/kg-day dose group.

Two-tailed t-tests, with error pooled across sex but not pooled across dose, were used to determine which combinations of dose group and exposure day showed a significant difference from baseline ( $p \leq 0.05$ ). Two-tailed t-tests, without pooled error, were used to determine which



combinations of dose group, exposure day and sex showed a significant difference from baseline ( $p \leq 0.05$ ).

**Table 3. Results from two-factor analysis of variance for TSH percent change**

Exposure Day	Source	SS	DF	SSE	DFE	F	P
2	Dose	1.76E+03	2	6.69E+03	17	2.23	0.1377
	Sex	1.66E+01	1	6.69E+03	17	0.04	0.8395
	Dose*Sex	1.60E+03	2	6.69E+03	17	2.04	0.1607
3	Dose	2.90E+03	2	7.52E+03	18	3.47	0.0532
	Sex	6.46E-01	1	7.52E+03	18	0.00	0.9691
	Dose*Sex	1.62E+03	2	7.52E+03	18	1.94	0.1726
4	Dose	1.40E+03	2	1.47E+04	17	0.81	0.4622
	Sex	1.99E+03	1	1.47E+04	17	2.29	0.1482
	Dose*Sex	2.70E+03	2	1.47E+04	17	1.56	0.2394
8	Dose	3.72E+03	2	3.58E+03	9	4.67	0.0407
	Sex	3.29E+02	1	3.58E+03	9	0.83	0.3872
	Dose*Sex	5.01E+02	2	3.58E+03	9	0.63	0.5551
14	Dose	3.19E+03	2	1.36E+04	15	1.76	0.2061
	Sex	7.30E+01	1	1.36E+04	15	0.08	0.7804
	Dose*Sex	1.65E+03	2	1.36E+04	15	0.91	0.4239
Post 1	Dose	4.69E+03	2	5.85E+03	18	7.22	0.0050
	Sex	2.66E+03	1	5.85E+03	18	8.18	0.0104
	Dose*Sex	2.73E+03	2	5.85E+03	18	4.19	0.0320
Post 15	Dose	6.59E+02	2	1.32E+04	18	0.45	0.6457
	Sex	8.02E+02	1	1.32E+04	18	1.09	0.3100
	Dose*Sex	6.06E+03	2	1.32E+04	18	4.12	0.0335

For TSH percent change at exposure day 8, there was a significant main effect of dose group ( $p = 0.0407$ ). Paired comparisons showed a significant difference between the 0.02 (mean = -1%) and 0.5 (mean = -39%) mg/kg-day dose groups.

For TSH percent change at post exposure day 1, there was a significant interaction between dose group and sex ( $p = 0.0320$ ). Simple main effect tests for each sex separately showed no significant effect of dose group for the males ( $p = 0.7188$ ) and a significant effect of dose group for the females ( $p = 0.0057$ ) with the 0.5 dose group (mean = -45%) significantly different from both the 0.02 dose group (mean = -2%) and the 0.1 dose group (mean = 13%). Also at post exposure day 1, there was a significant difference between males and females for the 0.02 dose group ( $p = 0.0132$ ) (mean: males = -34%, females = -2%) and the 0.1 dose group ( $p = 0.0363$ ) (mean: males = -27%, females = 13%) but not for the 0.5 dose group ( $p = 0.5405$ ).

For TSH percent change at post exposure day 15, there was a significant interaction between dose group and sex ( $p = 0.0335$ ). The only significant simple main effect was between males and females for the 0.1 dose group ( $p = 0.0064$ ) (mean: males = -16%, females = 40%).

**Table 4. Results from two-factor analysis of variance for T<sub>4</sub> percent change**

Exposure Day	Source	SS	DF	SSE	DFE	F	P
2	Dose	2.43E+02	2	1.06E+03	17	1.96	0.1721
	Sex	1.81E+02	1	1.06E+03	17	2.92	0.1056
	Dose*Sex	6.67E+01	2	1.06E+03	17	0.54	0.5940
3	Dose	2.53E+02	2	5.22E+03	18	0.44	0.6528
	Sex	3.22E+00	1	5.22E+03	18	0.01	0.9173
	Dose*Sex	1.08E+02	2	5.22E+03	18	0.19	0.8314
4	Dose	3.15E+02	2	1.78E+03	17	1.51	0.2491
	Sex	1.23E+01	1	1.78E+03	17	0.12	0.7361
	Dose*Sex	2.12E+02	2	1.78E+03	17	1.01	0.3842
8	Dose	7.43E+02	2	2.30E+03	9	1.45	0.2838
	Sex	4.88E+02	1	2.30E+03	9	1.91	0.2006
	Dose*Sex	3.50E+02	2	2.30E+03	9	0.68	0.5289
14	Dose	1.18E+03	2	4.83E+03	17	2.08	0.1554
	Sex	8.70E+01	1	4.83E+03	17	0.31	0.5871
	Dose*Sex	8.22E+02	2	4.83E+03	17	1.45	0.2628
Post 1	Dose	9.73E+02	2	4.65E+03	17	1.78	0.1990
	Sex	2.47E+02	1	4.65E+03	17	0.90	0.3555
	Dose*Sex	3.29E+02	2	4.65E+03	17	0.60	0.5590
Post 15	Dose	6.08E+02	2	4.86E+03	17	1.06	0.3670
	Sex	1.76E+02	1	4.86E+03	17	0.61	0.4438
	Dose*Sex	8.12E+02	2	4.86E+03	17	1.42	0.2689

**Table 5. Results from two-factor analysis of variance for free T<sub>4</sub> percent change**

Exposure Day	Source	SS	DF	SSE	DFE	F	P
2	Dose	9.73E+01	2	7.90E+03	17	0.10	0.9012
	Sex	2.60E+01	1	7.90E+03	17	0.06	0.8157
	Dose*Sex	1.55E+03	2	7.90E+03	17	1.66	0.2188
3	Dose	6.55E+01	2	5.97E+03	18	0.10	0.9065
	Sex	1.84E+01	1	5.97E+03	18	0.06	0.8167
	Dose*Sex	5.82E+02	2	5.97E+03	18	0.88	0.4330
4	Dose	2.05E+02	2	5.80E+03	17	0.30	0.7447
	Sex	1.80E+01	1	5.80E+03	17	0.05	0.8212
	Dose*Sex	7.37E+02	2	5.80E+03	17	1.08	0.3617
8	Dose	1.22E+02	2	3.45E+03	9	0.16	0.8554
	Sex	7.72E+01	1	3.45E+03	9	0.20	0.6645
	Dose*Sex	1.76E+02	2	3.45E+03	9	0.23	0.7997
14	Dose	4.91E+01	2	6.09E+03	14	0.06	0.9453
	Sex	3.65E+02	1	6.09E+03	14	0.84	0.3750
	Dose*Sex	2.85E+02	2	6.09E+03	14	0.33	0.7257
Post 1	Dose	8.53E+00	2	6.63E+03	18	0.01	0.9885
	Sex	2.08E+02	1	6.63E+03	18	0.56	0.4626
	Dose*Sex	1.13E+03	2	6.63E+03	18	1.53	0.2439
Post 15	Dose	4.16E+02	2	8.40E+03	18	0.45	0.6472
	Sex	2.83E+02	1	8.40E+03	18	0.61	0.4459
	Dose*Sex	1.54E+02	2	8.40E+03	18	0.17	0.8490

**Table 6. Results from two-factor analysis of variance for T<sub>3</sub> percent change**

Exposure Day	Source	SS	DF	SSE	DFE	F	P
2	Dose	1.17E+02	2	1.68E+03	17	0.59	0.5643
	Sex	1.68E+02	1	1.68E+03	17	1.70	0.2103
	Dose*Sex	2.20E+02	2	1.68E+03	17	1.11	0.3525
3	Dose	8.25E+01	2	1.96E+03	18	0.38	0.6901
	Sex	2.36E+01	1	1.96E+03	18	0.22	0.6470
	Dose*Sex	3.07E+02	2	1.96E+03	18	1.41	0.2699
4	Dose	3.85E+02	2	1.97E+03	17	1.66	0.2196
	Sex	1.42E+01	1	1.97E+03	17	0.12	0.7308
	Dose*Sex	6.39E+02	2	1.97E+03	17	2.76	0.0918
8	Dose	3.83E+02	2	1.87E+03	9	0.92	0.4315
	Sex	4.37E+00	1	1.87E+03	9	0.02	0.8878
	Dose*Sex	5.07E+02	2	1.87E+03	9	1.22	0.3390
14	Dose	2.09E+02	2	2.83E+03	17	0.63	0.5449
	Sex	1.49E+02	1	2.83E+03	17	0.89	0.3574
	Dose*Sex	3.68E+02	2	2.83E+03	17	1.11	0.3534
Post 1	Dose	6.77E+01	2	4.34E+03	18	0.14	0.8701
	Sex	2.14E+01	1	4.34E+03	18	0.09	0.7691
	Dose*Sex	6.90E+02	2	4.34E+03	18	1.43	0.2651
Post 15	Dose	6.32E+01	2	3.09E+03	17	0.17	0.8422
	Sex	1.82E+02	1	3.09E+03	17	1.00	0.3310
	Dose*Sex	3.04E+02	2	3.09E+03	17	0.84	0.4508

Figure 2 contains the mean percent change from baseline for each combination of dose group and exposure day. Means were averaged within each sex first and then averaged across sex. When comparing across exposure days within a dose group, keep in mind there were instances of missing data. No attempt was made to estimate missing data since all statistical tests were performed within an exposure day.

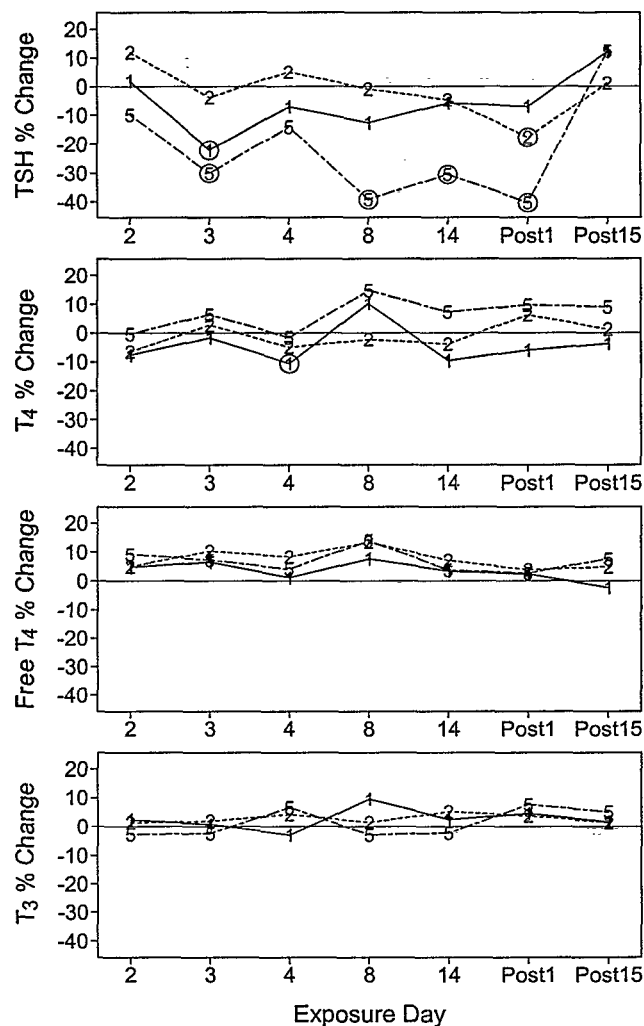


**Figure 2. Mean percent change from baseline. Legend: 2 = 0.02 mg/kg-day, 1 = 0.1 mg/kg-day, 5 = 0.5 mg/kg-day. Significant changes from baseline ( $p \leq 0.05$ ) are circled.**

Figure 3 contains the TSH mean percent change from baseline for each combination of sex, dose group and exposure day. The purpose of Figure 3 is to help interpret the significant Dose\*Sex interaction for TSH at post exposure day 1 and 15. Means from exposure day 14 were included to see the change from the last day of exposure into post exposure. Table 7 contains the data from each subject used to determine the means used in Figure 3.

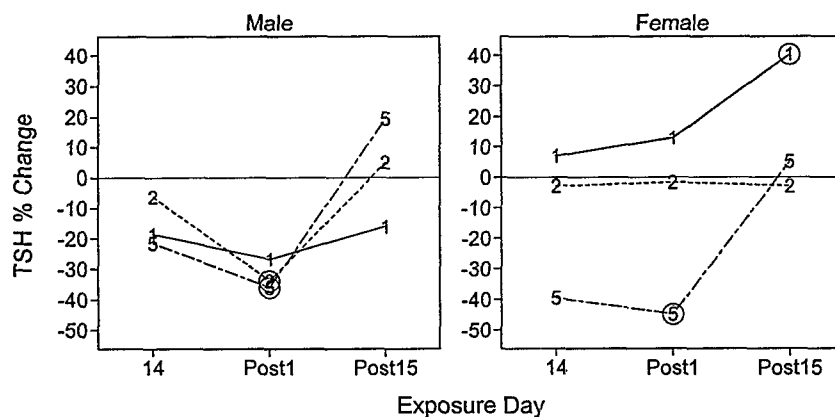


Figure 3. Mean percent change from baseline. Legend: 2 = 0.02 mg/kg-day, 1 = 0.1 mg/kg-day, 5 = 0.5 mg/kg-day. Significant changes from baseline ( $p \leq 0.05$ ) are circled.

Table 7. TSH percent change from baseline for each subject

Dose Group (mg/kg-day)	Sex	Subject	Exposure Day		
			14	Post 1	Post 15
0.02	M	A	-24	-27	-32
		B	-17	-36	8
		C	38	-28	15
		D	-23	-45	28
	F	E	-13	-20	27
		F	30	20	-45
		G	-25	-6	-9
		H		0	17
0.1	M	I	9	0	9
		J		-44	-33
		K	-40	-25	-40
		L	-25	-38	0
	F	M		27	27
		N	6	25	56
		O	-10	20	45
		P	25	-20	33
0.5	M	Q	-63	-54	-29
		R	-38	-52	8
		S	11	-21	63
		T	4	-17	35
	F	U	-65	-61	-25
		V	12	-18	18
		W	-50	-50	16
		X	-55	-51	13

Figure 4 and Table 8 contain the mean percent change from baseline for each combination of sex, dose group and exposure day. Figures 5 through 8 contain the percent change from baseline for each subject.

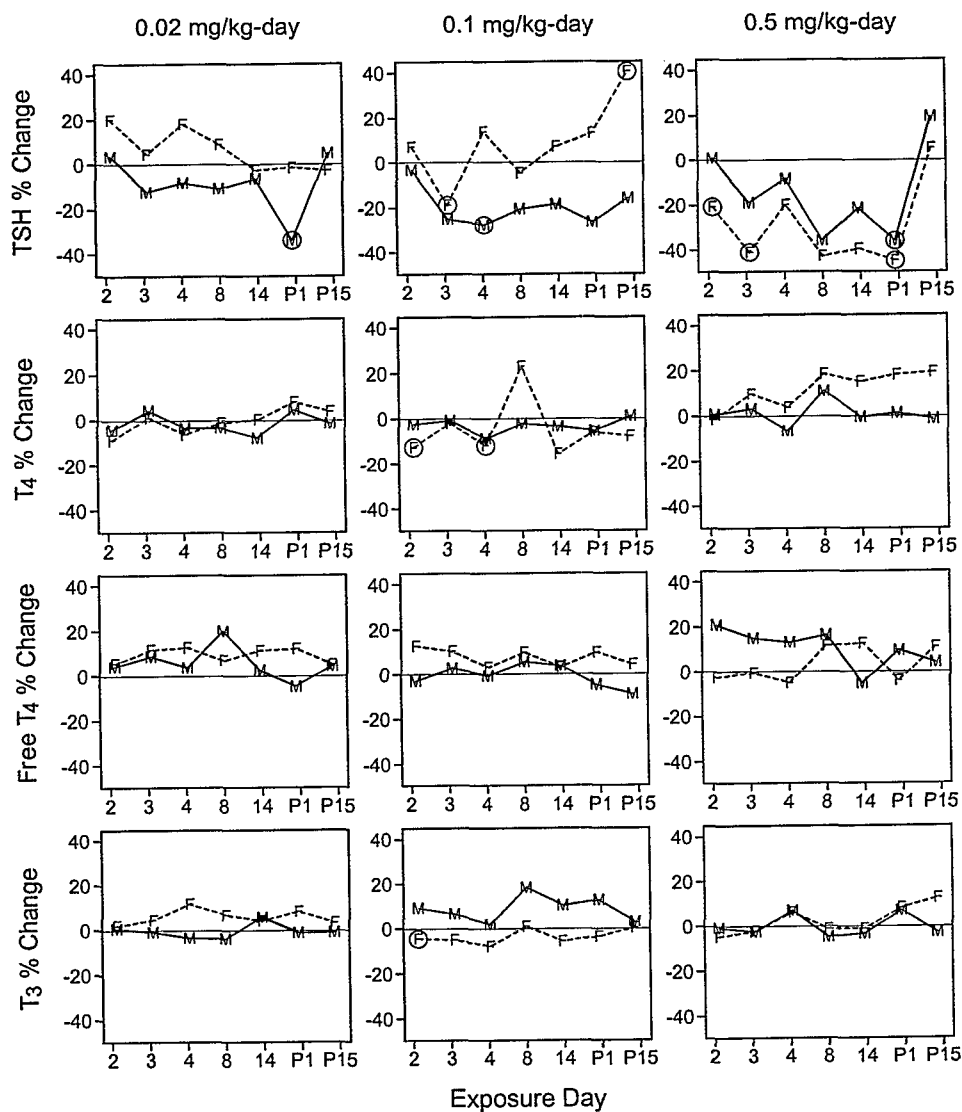


Figure 4. Mean percent change from baseline. Legend: M = Male, F = Female. Significant changes from baseline ( $p \leq 0.05$ ) are circled.

**Table 8. Mean and standard deviation of subjects for percent change from baseline**

Hormone	Dose mg/kg-day	Sex	Exposure Day						
			2	3	4	8	14	Post 1	Post 15
TSH	0.02	M	4 ± 9	-12 ± 27	-8 ± 14	-11 ± 4	-6 ± 30	-34 ± 8	5 ± 26
		F	20 ± 33	5 ± 25	18 ± 35	9 ± 23	-3 ± 29	-2 ± 17	-3 ± 32
		Avg	12 ± 22	-4 ± 26	5 ± 27	-1 ± 19	-5 ± 30	-18 ± 13	1 ± 29
	0.1	M	-3 ± 20	-25 ± 21	-28 ± 15	-21 ± 10	-19 ± 25	-27 ± 20	-16 ± 24
		F	7 ± 14	-19 ± 8	14 ± 50	-5 ± 18	7 ± 18	13 ± 22	40 ± 13
		Avg	2 ± 17	-22 ± 16	-7 ± 37	-13 ± 16	-6 ± 22	-7 ± 21	12 ± 19
	0.5	M	1 ± 27	-19 ± 25	-8 ± 22	-36 ± 29	-22 ± 35	-36 ± 20	19 ± 39
		F	-21 ± 9	-41 ± 5	-20 ± 21	-43 ± 10	-40 ± 35	-45 ± 19	5 ± 20
		Avg	-10 ± 20	-30 ± 18	-14 ± 22	-39 ± 24	-31 ± 35	-40 ± 19	12 ± 31
T <sub>4</sub>	0.02	M	-4 ± 8	4 ± 22	-3 ± 16	-3 ± 5	-8 ± 6	4 ± 20	-1 ± 8
		F	-9 ± 7	1 ± 9	-6 ± 12	-1 ± 8	0 ± 7	8 ± 21	4 ± 15
		Avg	-7 ± 7	3 ± 17	-5 ± 14	-2 ± 7	-4 ± 6	6 ± 20	1 ± 12
	0.1	M	-3 ± 12	-1 ± 20	-9 ± 8	-2 ± 23	-4 ± 16	-6 ± 10	1 ± 6
		F	-13 ± 4	-2 ± 11	-12 ± 4	23 ± 24	-16 ± 16	-6 ± 7	-8 ± 11
		Avg	-8 ± 9	-2 ± 16	-11 ± 6	10 ± 24	-10 ± 16	-6 ± 9	-4 ± 9
	0.5	M	1 ± 6	3 ± 18	-7 ± 3	11 ± 12	-1 ± 11	1 ± 12	-1 ± 14
		F	-1 ± 7	10 ± 18	4 ± 11	18 ± 14	15 ± 30	18 ± 21	19 ± 32
		Avg	0 ± 7	6 ± 18	-2 ± 8	15 ± 13	7 ± 23	10 ± 17	9 ± 24
free T <sub>4</sub>	0.02	M	4 ± 16	9 ± 10	4 ± 26	20 ± 0	3 ± 4	-5 ± 13	4 ± 13
		F	6 ± 10	12 ± 19	13 ± 25	7 ± 14	11 ± 13	12 ± 19	5 ± 16
		Avg	5 ± 14	10 ± 15	8 ± 25	13 ± 12	7 ± 9	4 ± 16	5 ± 14
	0.1	M	-3 ± 17	3 ± 18	-1 ± 14	6 ± 18	4 ± 13	-5 ± 11	-9 ± 11
		F	13 ± 26	10 ± 21	3 ± 14	10 ± 17	3 ± 26	10 ± 32	4 ± 31
		Avg	5 ± 22	6 ± 20	1 ± 14	8 ± 18	3 ± 22	2 ± 24	-2 ± 23
	0.5	M	21 ± 21	15 ± 20	13 ± 15	16 ± 21	-5 ± 13	9 ± 16	4 ± 12
		F	-3 ± 30	-1 ± 19	-5 ± 10	12 ± 35	13 ± 32	-4 ± 17	11 ± 34
		Avg	9 ± 26	7 ± 19	4 ± 12	14 ± 27	4 ± 26	3 ± 17	8 ± 26
T <sub>3</sub>	0.02	M	1 ± 7	-1 ± 13	-3 ± 13	-4 ± 3	6 ± 10	-1 ± 11	-1 ± 3
		F	2 ± 13	5 ± 4	12 ± 16	7 ± 3	4 ± 7	8 ± 13	3 ± 15
		Avg	1 ± 10	2 ± 9	4 ± 15	1 ± 3	5 ± 8	4 ± 12	1 ± 11
	0.1	M	9 ± 13	7 ± 11	2 ± 8	18 ± 16	10 ± 9	13 ± 9	3 ± 5
		F	-5 ± 2	-5 ± 6	-8 ± 7	1 ± 17	-6 ± 14	-4 ± 6	0 ± 7
		Avg	2 ± 10	1 ± 9	-3 ± 8	9 ± 17	2 ± 12	4 ± 8	2 ± 6
	0.5	M	-1 ± 9	-3 ± 14	7 ± 4	-5 ± 17	-3 ± 13	7 ± 17	-3 ± 8
		F	-5 ± 12	-2 ± 11	6 ± 10	-1 ± 21	-1 ± 19	8 ± 27	13 ± 26
		Avg	-3 ± 11	-2 ± 13	7 ± 8	-3 ± 18	-2 ± 16	8 ± 23	5 ± 19

**Note:** The standard deviation for the Avg row (average of males and females) is the pooled standard deviation across sex.

Although there were missing data in the original raw, there was only one value deleted for being considered an outlier. This was a TSH value for subject M (female, 0.1 mg/kg-day) on exposure day 14 reported as 133% change from baseline.

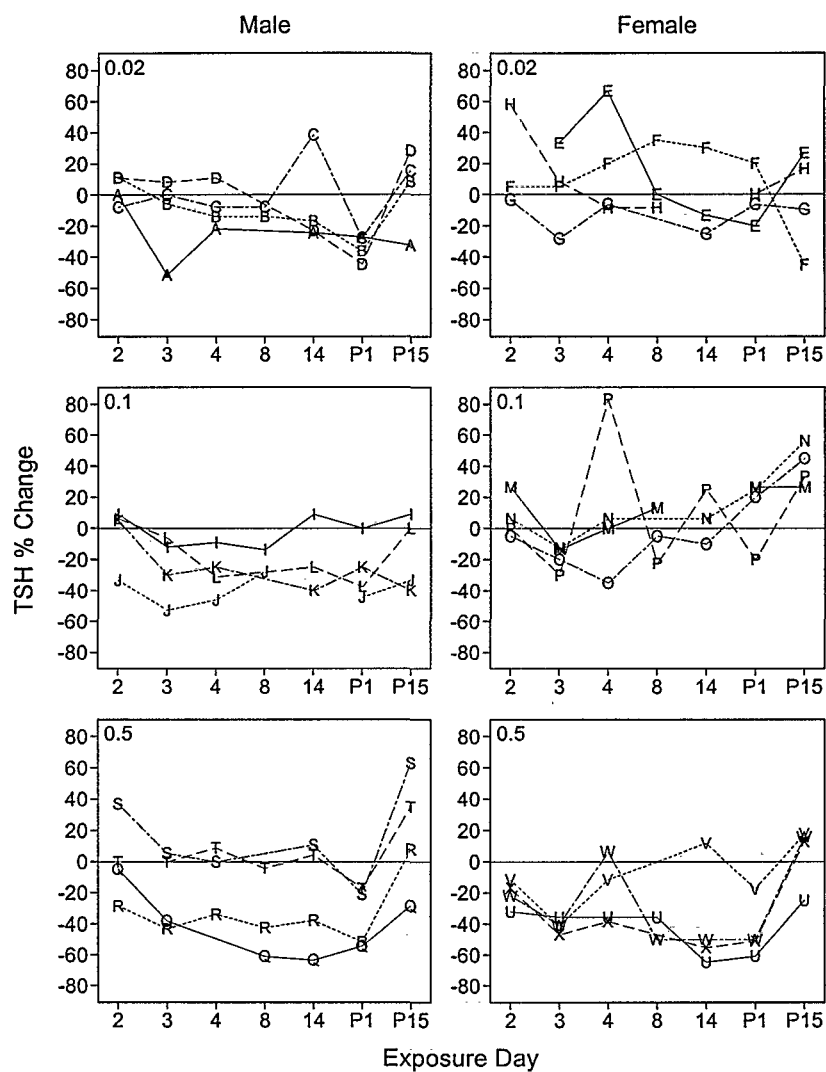


**Figure 5. Percent change in TSH from baseline for each subject (4 males and 4 females per dose group). The dose group is identified in the upper left corner of each plot.**



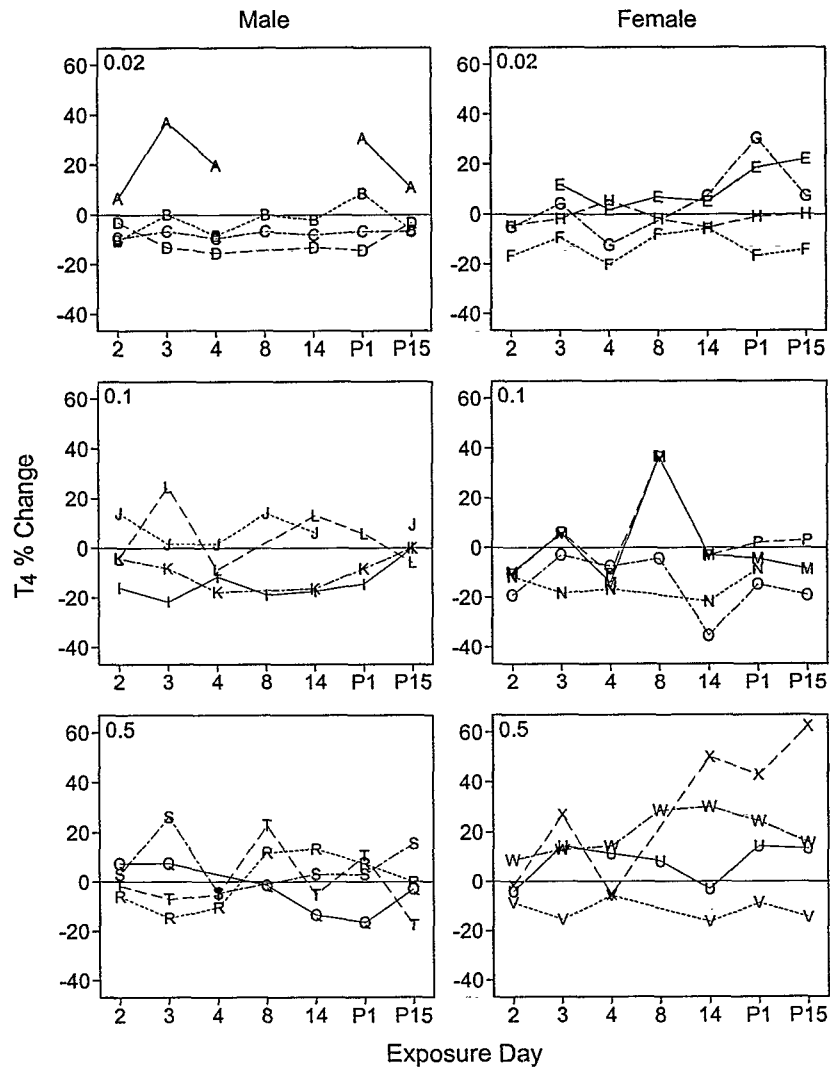


**Figure 6. Percent change in T<sub>4</sub> from baseline for each subject (4 males and 4 females per dose group). The dose group is identified in the upper left corner of each plot**

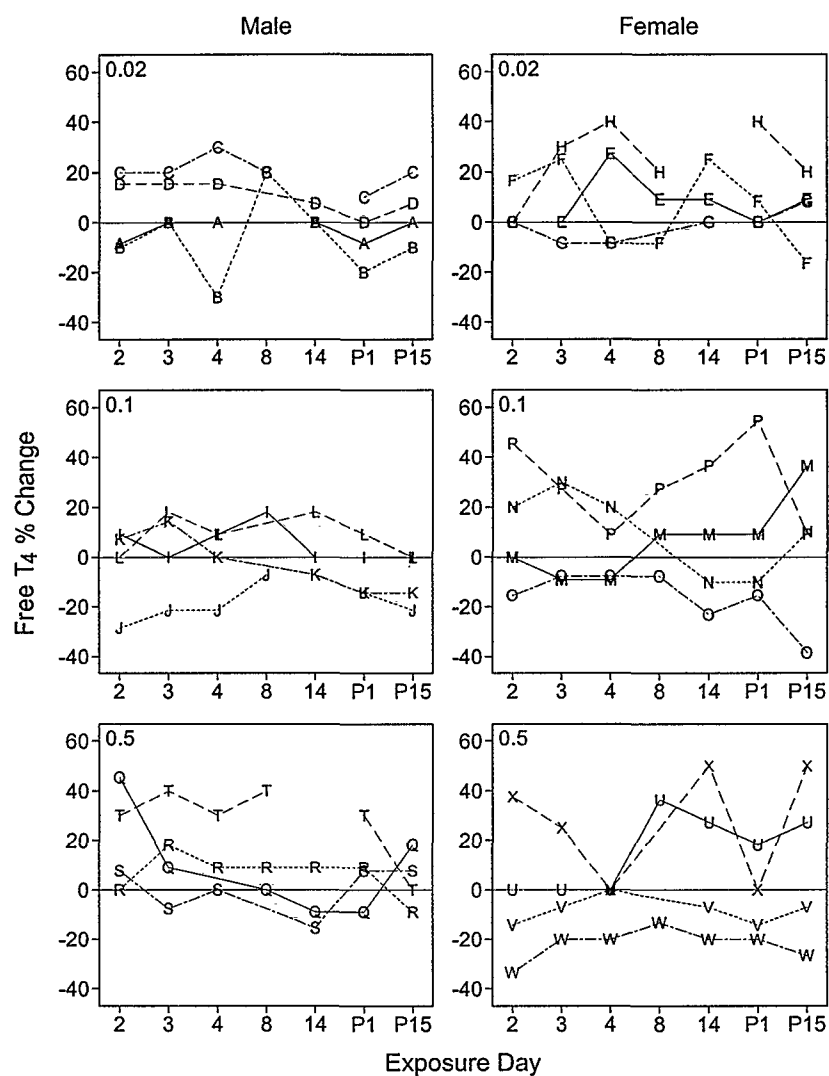


**Figure 7. Percent change in free T<sub>4</sub> from baseline for each subject (4 males and 4 females per dose group). The dose group is identified in the upper left corner of each plot.**

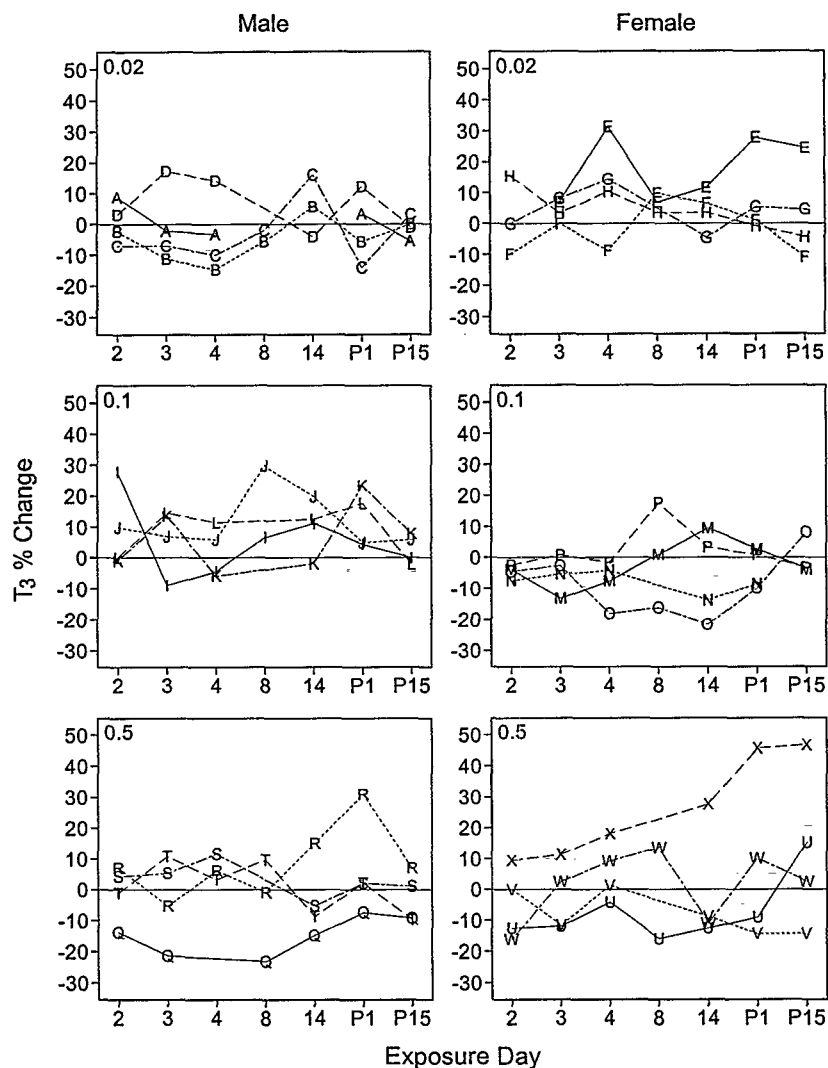


**Figure 8.** Percent change in T<sub>3</sub> from baseline for each subject (4 males and 4 females per dose group). The dose group is identified in the upper left corner of each plot.

### References

- Brabant, G., Prank, K., and Schofl, C., 1992a, Pulsatile patterns in hormone secretion: Trends.Endocrinol.Metab., 3, p. 183-190.
- Brabant, G., Bergmann, P., Kirsch, C.M., Kohrle, J., Hesch, R.D., and von zur Muhlen, A., 1992b, Early adaptation of thyrotropin and thyroglobulin secretion to experimentally decreased iodine supply in man: Metabolism, 41, p. 1093-1096.